Linköping Studies in Science and Technology
Dissertation, No. 1441

ZnO and CuO Nanostructures: Low Temperature Growth, Characterization, their Optoelectronic and Sensing Applications

Gul Amin

Linköpings universitet
INSTITUTE OF TECHNOLOGY

Physical Electronics and Nanotechnology
Department of Science and Technology (ITN)
Linköping University, SE-601 74 Norrköping, Sweden

ZnO and CuO Nanostructures: Low Temperature Growth, Characterization, their Optoelectronic and Sensing Applications

Gul Amin

ISBN: 978-91-7519-912-2
ISSN: 0345-7524

gul_phy@yahoo.co.uk
gul.amin@liu.se
Linköping University
Department of Science and Technology
SE-601 74 Norrköping
Sweden
Printed by LiU-Tryck, Linköping 2012.

ABSTRACT

One dimensional (1-D), zinc oxide (ZnO) and copper (II) oxide (CuO), nanostructures have great potential for applications in the fields of optoelectronic and sensor devices. Research on nanostructures is a fascinating field that has evolved during the last few years especially after the utilization of the hydrothermal growth method. Using this method variety of nanostructures can be grown from solutions, it is a cheap, easy, and environment friendly approach. These nanostructures can be synthesized on various conventional and nonconventional substrates such as silicon, plastic, fabrics and paper etc.

The primary purpose of the work presented in this thesis is to realize controllable growth of ZnO, CuO and nanohybrid ZnO/CuO nanostructures and to process and develop white light emitting diodes and sensor devices from the corresponding nanostructures.

The first part of the thesis deals with ZnO nanostructures grown under different hydrothermal conditions in order to gain a better understanding of the growth. Possible parameters affecting the growth such as the *pH*, the growth temperature, the growth time, and the precursors concentration which can alter the morphology of the nanostructures were investigated (paper 1). Utilizing the advantage of the low temperature for growth we synthesized ZnO nanostructures on different substrates, specifically on flexible substrates, which are likely to be integrated with flexible organic substrates for future foldable and disposable electronics (paper 2, 3).

In the second part of the thesis, using the results and findings from the growth of ZnO nanostructures, it was possible to successfully implement ZnO nanostructures for white light emitting diodes (LEDs) on different flexible substrates (paper 4, 5).

In paper 4 we realized a ZnO/polymer LED grown on a paper substrate. In paper 5 we extended the idea to print the ZnO nanorods/polymer hybrid LEDs with potential application to large area flexible displays.

In the last part of the thesis, CuO and nanohybrid ZnO/CuO nanostructures were utilized to fabricate Ag^+ detection and humidity sensors. In paper 6 we reported Ag^+ selective electrochemical sensor based on the use of functionalized CuO nanopetals. To combine the advantages of both oxides nanostructures and to improve the performance we fabricated a *pn*-heterojuction using intrinsic *n*-ZnO nanorods and *p*-CuO nanostructures which were then utilized as an efficient humidity sensor (paper 7).

Key words: Zinc oxide, Copper (II) oxide, Nanostructures, Hydrothermal growth, Light emitting diodes.

ACKNOWLEDGEMENT

I have made many new friends in the period of my Ph. D study. I would like to express my gratitude and appreciation for their help and support during these years, as well as friends from before, without their help and support this dissertation could not have been completed.

First and foremost I am grateful to my supervisor Prof. **Magnus Willander** for giving me the chance to work and study at *Physical Electronics and Nanotechnology group* at ITN/Linköping University. I can´t thank you enough for your ultimate effort, attention and valuable suggestions which were vital for my PhD work. From you, I learned the spirit of research -- to be productive, patient, novel, and to never give up when the situation is very tough --- I have learned a lot from you.

Secondly, I am thankful to my co-supervisor Associate Prof. **Omer Nour** for his encouragement and help during my study. He did not only support me in study but also helped me a lot whenever I need to translate letters from Swedish to English.

Thirdly, I also thank all my co-authors especially Ahmad Zainelabdin, Saima Dr. M. O. Sandberg, and Dr. Asif for the valuable input, without you this project would have been impossible.

I would also like to thank Ann-Christin Norén, and Sophie Lindesvik for being efficient and always helpful administrators.

I also acknowledge the support and facilities provided by the ITN/ University of Linköping and my department in Pakistan throughout my Ph.D.

I am thankful to all past and especially all present members of the *Physical Electronics and Nanotechnology research group* for their moral support, good wishes and memorable days shared together. I want to give a special note for few people that I've discussed research and other things of interest with; Haleem, Kamran, Zia Ullah, Dr. Owais, Dr. Adnan, Usman and Arif.

Last but not least, I would like to thank my wife and my daughter Perisha Khan for their love and support I hope I have not taken for granted your patience during early days when I spent more time in university/lab than at home. I am grateful to my family, parents and parents-in-law for their support, understanding and invaluable prayers.

To anyone I have forgotten to acknowledge in this text: Thank you!

Gul Amin

LIST OF PUBLICATIONS

Papers included in this dissertation:

Paper 1 **G. Amin,** M. H. Asif, A. Zainelabdin, S. Zaman, O. Nur, and M. Willander, "Influence of *pH*, precursor concentration, growth time, and temperature on the morphology of ZnO nanostructures grown by the hydrothermal method", *Journal of Nanomaterials, 10, No. 269692 (2011).*

Paper 2 A. Zainelabdin, S. Zaman**, G. Amin**, O. Nur, and M. Willander, "Deposition of well-aligned ZnO nanorods at 50 ^{o}C on metal, semiconducting polymer, copper oxides substrates and their structural and optical properties", *Crystal Growth & Design, 10, 3250-3256 (2010).*

Paper 3 **G. Amin**, I. Hussain, S. Zaman, N. Bano, O. Nur, M. Willander, "Current-transport studies and trap extraction of hydrothermally grown ZnO nanotubes using gold Schottky diode", *Physica Status Solidi A 207, 748-752 (2010).*

Paper 4 **G. Amin,** S. Zaman, A. Zainelabdin, O. Nur, and M. Willander, "ZnO nanorods–polymer hybrid white light emitting diode grown on a disposable paper substrate", *Phys. Status Solidi RRL 5, 71–73 (2011).*

Paper 5 **G. Amin**, M. O. Sandberg, A. Zainelabdin, S. Zaman, O. Nur, M. Willander, "Scale-up synthesis of ZnO nanorods for printing inexpensive ZnO/Polymer white light emitting diode", *Journal Materials Science. 47, 4726-4731 (2012).*

Paper 6 **G. Amin,** M. H. Asif, A. Zainelabdin, S. Zaman, O. Nur, and M. Willander, "CuO nanopetals based electrochemical sensor for selective Ag^{+} measurements", *Sensor Letters. 10, 1-6 (2012).*

Paper 7 A. Zainelabdin, **G. Amin,** S. Zaman**,** O. Nur, J. Lu, L. Hultman, and M. Willander, "CuO/ZnO nanocorals synthesis via hydrothermal technique: growth mechanism and their application as humidity sensor" *Journal of Materials Chemistry DOI: 10.1039/C2JM16597j (2012).*

The author has also been involved in the following papers not included in this thesis.

[1] M. Riaz, A. Fulati, **G. Amin**, N. H. Alvi, O. Nur, and M. Willander, ''Buckling and elastic stability of vertical ZnO nanotubes and nanorods'' *J. Appl. Phys. 106, 034309 (2009).*

[2] A. Fulati, S. M. Usman Ali, M. Riaz, **G. Amin**, O. Nur and M. Willander, ''Miniaturized pH Sensors Based on Zinc Oxide Nanotubes/Nanorods'', *Sensors. 9(11), 8911-8923 (2009).*

[3] A. Zainelabdin, S. Zaman, **G. Amin**, O. Nur, and M. Willander, ''Stable white light electroluminescence from highly flexible polymer/ZnO nanorods hybrid heterojuction grown at 50 ^{o}C'' *Nanoscale Res. Lett. 5:1442–1448 (2010).*

[4] M. Willander, O. Nur, S. Zaman, A. Zainelabdin, **G. Amin**, J. R. Sadaf, M. Q. Israr, N. Bano, I. Hussain , and N. H. Alvi, ''Intrinsic White Light Emission from Zinc Oxide Nanorods Heterojuction on Large Area Substrates'', *Proc. of SPIE . 7940 79400 A (2011).*

[5] S. Zaman, A. Zainelabdin, **G. Amin**, O. Nur, and M. Willander, "Effect of the Polymer Emission on the Electroluminescence Characteristics of n-ZnO Nanorods/p-Polymer Hybrid Light Emitting Diode", *Applied Physics A. 104:1203–1209 (2011).*

[6] S. Zaman, M. H. Asif, A. Zainelabdin, **G. Amin**, O. Nur, and M. Willander, CuO nanoflowers as an electrochemical *pH* sensor and the effect of *pH* on the growth'', *Journal of Electroanalytical Chemistry. 662, 421–425 (2011).*

[7] M. Willander, K. Ul Hasan, O. Nur, A. Zainelabdin, S. Zaman and **G. Amin**, "Recent progress on growth and device development of ZnO and CuO nanostructures and graphene nanosheets", *J. Mater. Chem. 22, 2337-2350 (2012).*

[8] M. Willander, O. Nur, G. Amin, A. Zainelabdin and S. Zaman "Zinc Oxide and Copper Oxide Nanostructures: Fundamentals and applications", MRS Fall meeting DOI: 10.1557/opl.2012.65.

[9] S. Zaman, A. Zainelabdin, **G. Amin**, O. Nur and M. Willander, "Efficient catalytic effect of two-dimensional petals and three-dimensional flowers like CuO nanostructures on the degradation of organic dyes", *Submitted to J. Phys and Chem. Solids.*

[10] A. Zainelabdin, S. Zaman, **G. Amin**, S. Hussain, O. Nur, M. Willander, "The growth of CuO/ZnO Composite Nanostructures: Hydrothermal Mechanisms, Precursor's Effects, and their Optical Properties", *Submitted to Acta Materialia*.

[11] A. Zainelabdin, S. Zaman, **G. Amin**, S. Hussain, O. Nur, M. Willander, "Optical and current transport properties of CuO/ZnO nanocorals p-n heterostructures hydrothermally synthesized at low temperatures", *Submitted to Appl. Phys. A.*

[12] A. Zainelabdin, O. Nur, **G. Amin**, S. Zaman, and M. Willander, "Metal Oxide Nanostructures and White Light Emission", *Proc. of SPIE*. 8263, 82630N (2012).

[13] S. Zaman, A. Zainelabdin, **G. Amin**, O. Nur, and M. Willander, "Influence of the polymer concentration on the electroluminescence of ZnO nanorods/polymer hybrid light emitting diode" (Manuscript).

Patent

Title: Rectifying and electroluminescent devices manufactured by printing.

M. O. Sandberg, **G. Amin**, and M. Willander (*Pending).*

Contents

1 Introduction

Here, in the first chapter of the thesis, I will briefly introduce the relevant concepts, some basic information in nanotechnology, nanostructures and nanomaterials. Some essential questions will be answered through literature survey, including differences between nanostructured and bulk materials, advantages and fabrication challenges of nanomaterials. Different low-dimensional nanostructures will be introduced with focus on zinc oxide (ZnO) and cupric oxide (CuO) nanostructures, which are the two materials studied in this thesis, followed by their nanohybrid structure.

1.1 Nanotechnology and low-dimensional nanostructures

As we entered the twenty-first century, nanotechnology is revolutionizing many areas e.g. electronics, optoelectronics, sensing and so on, resulting in overwhelming publications in many journals across different fields. The Buzzword “nanotechnology” used in 1980 for the first time is now around us everywhere. Fundamentally, nanotechnology involves the creation and manipulation of typical functional materials, devices and systems that fall in the range of 1–100 nm [1]. When this fact occurs exclusively in one dimension, we call it a thin-film or surface, whereas in two dimension, nanorods, nanotubes, and other attractive morphologies can be formed. Materials that are at the nanoscale in three dimensions are nanoparticles [2]. ZnO and CuO have rich family of nanostructures and can be grown in zero-dimensional (0D), one-dimensional (1D), and two-dimensional (2D) morphologies, (geometrical illustration of different dimensions is shown in Figure 1.1), while a three-dimensional (3D) structure representing the bulk. In 0-D nanostructures like quantum dots the carriers are confined in all the three directions, unlike in nanorods and thin films where carriers can freely move in one and two directions respectively, while in bulk structures the carriers are free in all three direction. The density of states (DOS) (number of electronic states per unit volume and energy) is greatly modified for

different type of nanostructures depending on the degree of confinement as shown in Figure. 1.1. For materials in the bulk form, the DOS has a square root dependence on energy and this dependence changes accordingly with the dimensionality of the quantum structures as seen from Figure. 1.1. The variation in DOS with dimensionality results in outstanding optical and electrical properties for realizing advanced nanodevices.

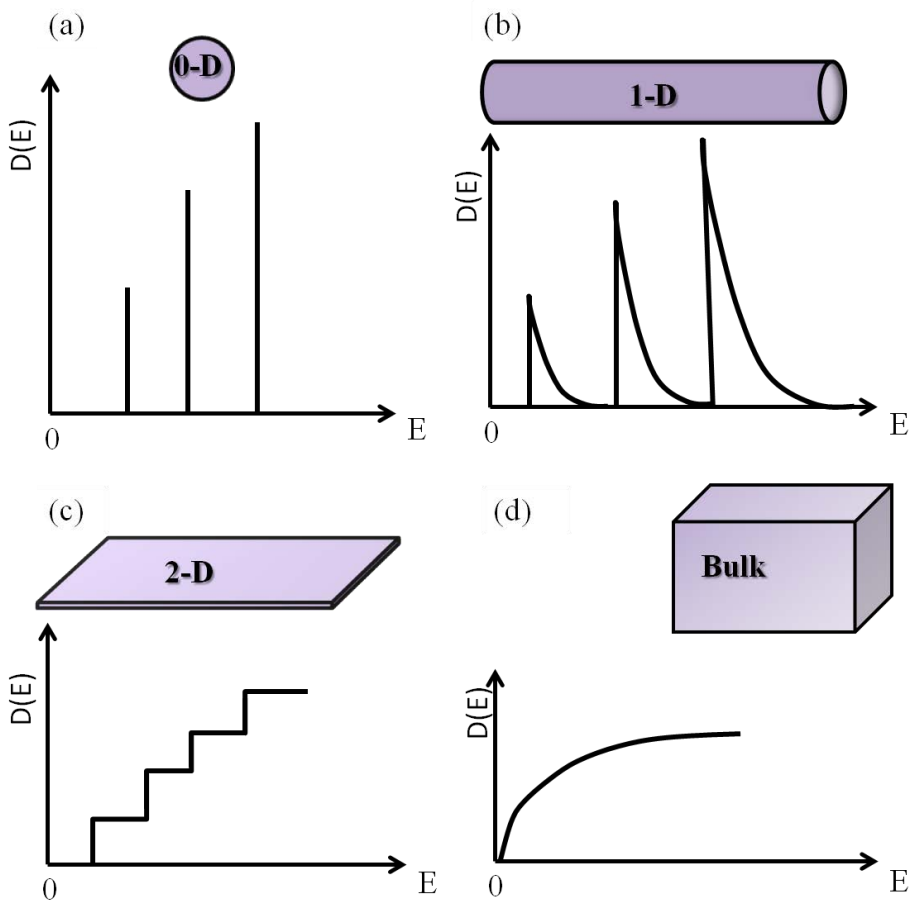

Figure 1.1: *Schematic representation of: (a) 0-dimension (0-D), (b) 1-dimension (1-D), (c) 2-dimension (2-D) and (d) 3-dimension(3-D). The corresponding density of states (DOS) plots for each type is also presented.*

In an effort to increase integration, enhance functionality, and reduce energy consumption, the major focus of the development of semiconductor devices was on miniaturization. As a result, semiconductor devices have evolved from millimeter-sized devices down to nanometer-sized devices. In this regard, the development of different synthesis methods capable of realizing high crystallinty and purity of materials is an enabling step toward making such nano-devices a reality. Materials in the nanometer scale still preserve many properties in the same way as that of bulk form e.g. the crystal structure and the lattice constant remain the same at the nano-scale, as confirmed by x-ray diffraction (XRD) and transmission electron microscope (TEM). However, significant characteristics of nanostructures are their high surface to volume ratio, spatial confinement, which leads to exhibit novel electrical, optical, chemical, and mechanical properties distinctively different from that of the bulk. With great reduction in particle sizes, a number of statistical and quantum mechanical phenomena become pronounced altering the electronic and optical properties of materials, as the de Broglie wavelength of carriers are comparable at this scale to the dimensions of the nanostructures. Therefore the synthesis of different nanostructures and exploiting their extraordinary properties became the goal and dream of researchers. Nanostructured materials are those with at least one dimension falling in the nanometer scale, including nanoparticles (quantum dots, when exhibiting quantum effects), nanorods and nanowires, thin films, and bulk materials made of nanoscale building blocks or consisting of nanoscale structures. Recent decades have witnessed the synthesis of a wide variety of nanoscale materials of different sizes, shapes and compositions. The interest in nanomaterials is driven by their many desirable properties. In particular, the ability to tailor the size and structure and hence the properties of nanomaterials offer excellent prospects for designing novel optoelectronic and sensing nanodevices with performance beyond what can be established at the bulk level.

In the emerging fields of nanotechnology metal oxides nanostructures stand out as being among the most versatile because of their excellent physical and chemical properties. One dimensional (1-D) metal oxide

semiconducting nanostructures such as ZnO [3-5], titanium oxide (TiO_2) [6], and CuO [7, 8] have gained a leading edge in most active areas of technological applications due to their unique performance in optoelectronics, catalysis, and sensing [9, 10]. Thus, metal oxides are attracting significant attention of many researchers in different fields to develop new, easy, inexpensive, and effective methods to control and prepare nanoscale metal oxides, and metal oxide polymer composites.

1.2 Properties of zinc oxide and copper oxide

1.2.1 Zinc oxide (ZnO)

The emphasize here will be on the fundamental properties of ZnO, like growth, electrical and optical properties, since the potential for optoelectronic devices based on ZnO is also one of the main motivations for the present work. ZnO is a direct wide band-gap (3.37 eV at room temperature) II-VI binary compound semiconductor and crystallizes in three forms: hexagonal wurtzite, cubic zincblende, and the rarely observed cubic rocksalt [11]. The hexagonal wurtzite structure of ZnO is the most common phase having a crystal structure C_{6v} or $P6_3mc$, which occurs almost exclusively at ambient conditions [12, 13]. The wurtzite ZnO structure consists of alternating zinc (Zn) and oxygen (O) atoms is shown in Figure 1.2. The ZnO structure has polar surface (0001) which is either Zn or O terminated and non-polar surfaces (1120) and (1010) possessing an equal number of both atoms. The polar surface of ZnO is highly meta-stable in nature and is responsible for several unique and astonishing properties including piezoelectric properties, it also play a key role in column growth, favorable for etching due to higher energy. The polar surface is also known to possess different physical and chemical properties [14].

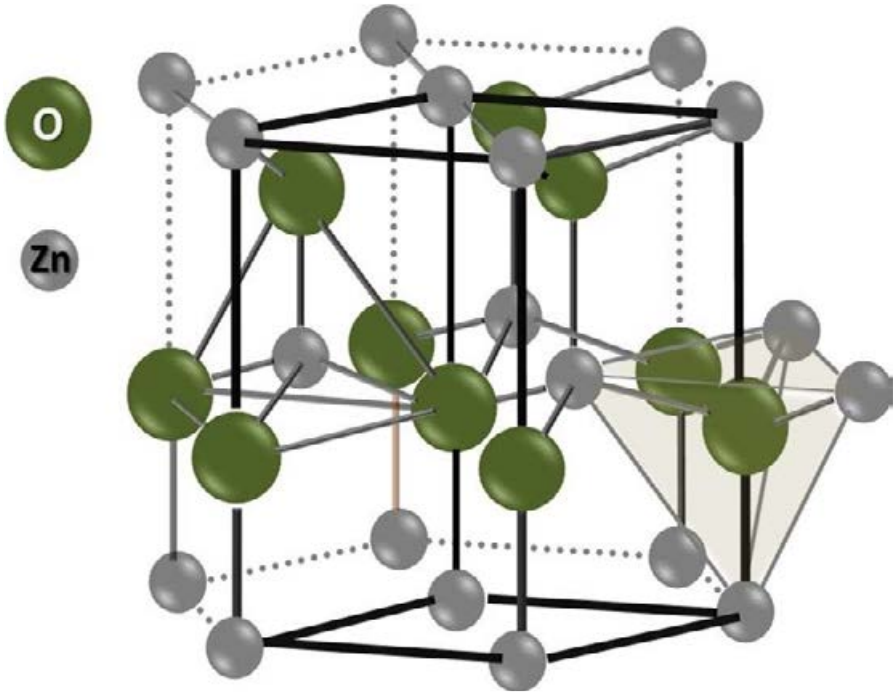

Figure 1.2: *Crystal structure of hexagonal wurtzite ZnO.*

Direct band gap materials have intrinsically high luminescence yield compared to indirect band gap materials and increase in the band-gap reduces the leakage current of the devices and their temperature dependence significantly [12, 15]. Among the II-VI semiconductors, ZnO has relatively higher and stable exciton binding energy of 60 meV at 300 K, almost three times larger than its competitor GaN which has an exciton binding energy of 25 meV. It is also one of the reasons that ZnO is so attractive for optoelectronic devices. Higher exciton binding energy materials give brighter emissions, because exciton is already a bound system, which radiatively recombine with high efficiency without requiring traps to localize the carriers [12, 15]. Other favorable aspects of ZnO are that it is non-toxic, cheap, relatively abundant source materials, and chemically stable. It can be synthesized as a large single crystal by various methods and it can be grown in various morphologies and dimensions. ZnO nanostructures are promising candidates in miniaturized optoelectronics and sensing devices. By alloying,

the band-gap can be tuned further into the UV or down into the green spectral ranges i.e. from 2.8 to 4 eV [16]. A tendency of different fast growth directions of ZnO could result in growth of a diverse group of hierarchical and complex nanostructures. This is partly reflected by the various structural morphologies of ZnO nanomaterials such as nanorods, nanotubes, nanocorals, nanoflowers, and nanowalls. These unique nanostructures show that ZnO probably has the richest family of nanostructures among all known materials which demonstrate potential for its diverse practical applications in the near future. In particular, 1-D ZnO nanorods are potentially useful for various nanodevices such as light emitting diodes (LEDs), chemical sensors, solar cells, and piezoelectric devices, because of their high aspect ratio and large surface area to volume ratio ensure high efficiency and sensitivity in these applications. Furthermore, ZnO is bio-safe and biocompatible and may be used for biomedical applications without coating. Some of the common properties of the ZnO bulk materials are listed in Table 1.1.

Table 1.1: *Key properties of bulk wurtzite ZnO*

Property	**Value**	**Reference**
Lattice parameters	a = b =3.25 Å c = 5.21 Å u =0.348 c/a =1.593-1.6035	[11, 14, 17]
Density	5.606 gm/cm^3	[14]
Melting point	2248 K	
Stable crystal structure	Wurtzite	[14]
Dielectric constant	8.66	[18]
Refractive index	2.008	[19]
Band gap (E_g)	3.37 eV, (direct)	[14, 20]
Exciton binding energy	60 meV	[21]
Electron/Hole effective mass	0. 24 m_o / 0. 59 m_o	[17]
Hole mobility (300K)	5-50 $cm^2/V\,s$	[22]
Electron mobility (300K)	100-200 $cm^2/V\,s$	[22]

1.2.2 Copper (II) oxide

Among other compound semiconductors, copper oxide is of great interest in semiconductor physics. Copper forms two well-known stable oxides, cupric oxide (CuO) and cuprous oxide (Cu_2O). These two oxides have different physical properties, different colors, crystal structures and electrical properties. There are many reasons why CuO is chosen for sensing applications. CuO has monoclinic structure belong to space group 2/m, it displays a wealth of interesting properties, it is abundant, non-hazardous source materials, and it can be prepared by low cost solution methods which are the key issues for sensing applications. Figure 1.3 shows the monoclinic structure of the CuO.

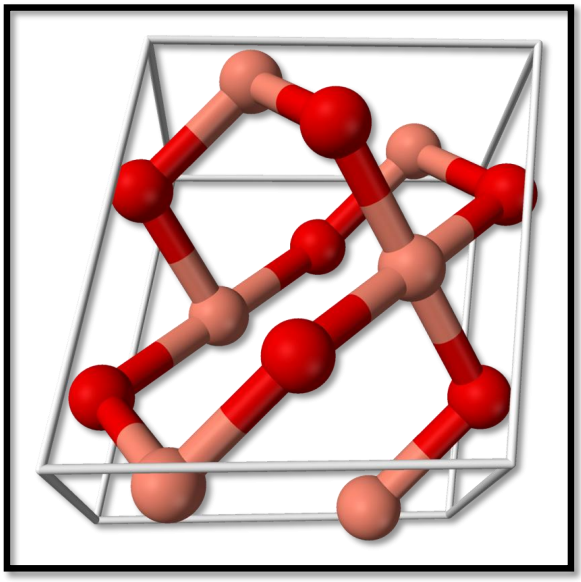

Figure 1.3: *Copper (II) oxide (CuO) crystal structure [23].*

It is a direct band-gap p-type semiconductor with a narrow band gap of around 1.2-1.55 eV in bulk [24]. The possibility of low cost production methods and the good electrochemical properties make CuO to be one of the best materials for electrical, optical, sensing and so forth. As mentioned before, nanostructures exhibit many features that are not

present in bulk material because of e.g. their high surface area to volume ratio. CuO nanostructures have a wide range of applications [25]. These include catalysis and gas-sensing where the surface area enhancement is particularly important. Some of the key properties of the CuO bulk materials are listed in Table 1.2.

Table 1.2: *Key properties of CuO at room temperature (300 K)*

property	Value	Reference
Lattice constants (300K)	a = 4.68 Å b = 3.42 Å c = 5.13 Å	[17, 26]
Density	6.31gm/cm^3	[24]
Melting point	1975 ^oC	[24]
Stable phase at 300 K	Monoclinic	[26]
Dielectric constant	18.1	[24]
Refractive index	1.4	[24]
Band gap (E_g)	1.21-1.55eV, direct	[27]
Hole effective mass	0. 24 m_o	[17]
Hole mobility	0.1-10 $cm^2/V\,s$	[24]

1.3 Purpose and outline of the thesis

The work presented here serves to address the fabrication of semiconductor oxide nanostructures and evaluate their potential for light emitting diodes (LEDs) and sensing applications. The work has been carried out with two different types of oxides nanomaterials.

Specifically, the objectives of this dissertation are as follows:

1) The main motivations have been to optimize and develop the individual ZnO and CuO fabrication processes with regards to attain

rational control over nanostructures morphology, preferred orientation, and high level of crystallinty.

2) Characterize and study structural, optical and electrical properties of ZnO, CuO and their nanohybrid structures.

Characterization of ZnO, CuO and ZnO/CuO nanohybrid structures will be beneficial in understanding the growth behavior of these nanostructures. The morphology and crystalline structure of CuO and ZnO nanostructures were investigated using scanning electron microscopy (SEM), atomic force microscopy (AFM) and x-ray diffraction (XRD). The existence of a high degree of long range order (crystallinty) was sought in order to maximize the charge carrier mobility, and thus to enhance the device performance. It has been reported that high levels of preferred orientation serve to lower the ZnO resistivity due to reduction in the scattering phenomena at the grain boundaries and the shorter carrier path lengths encountered by carriers travelling along the c-plane [28, 29].

3) Realize and demonstrate solution-processable inorganic/polymer LEDs on different non-conventional flexible and disposable substrates for the application of large area devices.

With the optimization of ZnO fabrication processes, steps were taken to integrate ZnO nanorods into flexible hybrid LEDs. To realize the advantage of flexible devices, nanostructures synthesized via low temperature hydrothermal methods are strongly desirable. Moreover, aligned ZnO nanorods will enhance the performance of LEDs because of the internal reflection established between the ZnO and the polymer layers. In addition, we also printed ZnO nanorods which serves to further increase the performance of the inorganic/polymer LEDs. Despite successful demonstrations of mechanically flexible pure organic devices, however, they are generally sensitive to working conditions and are unstable during long term operation [30].

4) Incorporate the optimized CuO nanostructure into electrochemical sensor for the detection of silver ions (Ag^{+}) and to monitor the response of the sensor.

Our group has performed extensive studies on different metal ions detection e.g. Na^+, Ca^+ by using n-type ZnO nanostructures with the aim to produce a proto type electrochemical extra/intra cellular biosensors [31-33]. CuO is also known to be capable of having high sensing properties, so the idea was to carry out the measurement with p-type semiconducting CuO nanostructures, as it may lead to high sensitivity and rapid response time sensor.

5) To investigate and develop novel p-CuO/n-ZnO heterostructures that may further increase the device interfacial area and response time of the humidity sensor.

As stated above, the combination of ZnO and CuO structures allow for the creation of novel sensor designs. The hydrothermal growth method has been employed in the fabrication of a unique CuO/ZnO heterostructures. This device is comprised of ZnO nanorods among a matrix of CuO nanopetals. Consequently, the area of the heterostructures interface is greatly increased and diffusion paths are essentially negligible.

The outline of this thesis is as follows: First introduction of the field, including some properties of the ZnO and the CuO materials is presented. This is followed by a chapter describing the status and literature related to inorganic/polymer LEDs and sensing studies in this work. After this, the synthesis of materials for the growth of different morphologies and device fabrication are presented. In addition, a chapter on the characterization tools used in this work is also included. Finally, conclusions evident from experimental results are summarized followed by short outlook, which hopefully will encourage future work in this field. This is then followed by the appended papers.

2 Status and Development of ZnO and CuO Devices

The following chapter is designed so as to give a brief overview of the ZnO-polymer hybrid LEDs, CuO nanostructures used as an electrochemical sensor materials and nanohybrid structures of both n-ZnO and p-CuO utilized as a humidity sensor.

2.1 ZnO-polymer hybrid LEDs

The history of LEDs goes back to 1907, when light emission from a silicon carbide (SiC) was first reported by H. J. Round [34]. At that time, the potential of the technology was not realized and the discovery largely remained unnoticed. It was not until in 1962 when first practical visible (red) *p-n* LED was discovered by Holonyak from general electric company and is known as the "the father of the light emitting diode" [35]. However, after that LEDs research got wide attention and is used in numerous signaling and display applications. In 1995 Nakamura demonstrated first blue LED based on InGaN, and used coating with phosphor to mix other color with blue to produce white LEDs; he was awarded Nobel Prize in 2006. Nowadays LEDs of almost every color are available with reasonable efficiency which opens the opportunity to use LEDs in areas beyond conventional usage and signal applications. Now LEDs can be used in high-power applications thereby enabling the replacement of conventional light sources. The LEDs technology have numerous advantages over the traditional incandescent and fluorescent lamps, such as smaller size, long lifetime, robustness, fast switching and high efficiency [36]. LEDs based light sources have potential to replace the wide spread conventional lamps which will lead to decrease in power consumption worldwide by many orders and will also decrease the environmental pollution threats. The life time of incandescent sources (~ 500 h) and fluorescent sources (~ 5000 h) is far less than the LEDs (>10^5 h) [36]. LEDs devices are more compact, more durable and capable to change color in real time, and are finding more applications in domestic, commercial and industrial environments.

White light is the type of light with the most universal applications. However, so far, white LEDs are typically made either by the RGB-method using three LEDs or the phosphor-converted LED i.e. starting from a blue emitting LED and converting part of its light to green and red using phosphor materials. There is a need to look for white LEDs from a single device with emission spectrum covering the entire visible range to accurately render all colors, with absence of harmful radiation emission. At the same time they should be cheap, an excellent chemical and temperature stable, current driving and high color quality white LEDs.

In general LEDs can be divided into two categories; (i) homojunction and (ii) heterojuction LEDs. The application of homojunction ZnO LEDs has been hindered due to the difficulties inherent in fabrication of a reliable, stable, reproducible and device quality p-type ZnO material. In spite the fact that the development of p-type doping of ZnO recently progressed at a rapid pace and many research articles are reported from time to time claiming to have produced p-ZnO [37-43]. But in the ZnO research community it is still a perception that all such claim have flaws as not being reproducible by others, especially those results quoting stable and heavy doping, or high mobility. However, there are always many ways around the problems and thus much effort has been devoted to find an alternative solution. To circumvent this problem, an interesting and effective way is to develop hybrid *p*–*n* heterojuction LEDs, which are composed of heterojuction between n-ZnO and other p-type materials. A number of different p-type materials have been used to produce ZnO-based working LEDs in which ZnO function as an n-type active component, and a large variation in device performance has been reported [44]. Compared to thin films, nanorods-based LEDs are expected to result in an improved device performance [45-47]. The amplified performance in ZnO nanorods based devices is presumed infect that well crystalline and well facet nanorods will serve as an active and self contained optical cavities as illustrated in Figure 2.1. However, device performance will also be strongly dependent on the material properties of the nanostructures. Since, ZnO has a large number of deep level defects, which emit light covering the visible spectral range and were attributed to various defects including

violet, blue, green, yellow, and red [43, 48], but the defect emission origin is still controversial [48-50]. Since the native defects observed in ZnO samples fabricated under different conditions significantly affect the optical and electronic properties of ZnO, they are expected to significantly affect the performance of ZnO-based optoelectronic devices, such as light-emitting diodes (LEDs) [50].

In addition to the effect of native defects on ZnO properties, defects at the interface of the heterojuction are expected to affect the performance of an LED. Variation in material properties and interface properties in ZnO-based devices is likely the cause of the large spread of reported turn-on voltages and emission colors in ZnO-based heterojuction LEDs. Thus, there is a considerable interest in studying the influence of ZnO properties and device architecture (choice of the p-type material, buffer/interface layers, etc.) on the LED performance. Heterojuction LEDs were successfully demonstrated on different conventional substrates such as GaN [51], SiC [52]. On the other hand, by taking the low temperature manufacturing advantage of ZnO nanostructures, which is compatible with temperature sensitive flexible plastic or paper substrate, it was also hybridized with different p-type polymers such as polymer polyvinyl carbazole (PVK)[53, 54], *N*,*N*′-di(naphth-2-yl)-*N*,*N*′-diphenylbenzidine (NPB) [55], poly [2-methoxy-5-(2’-ethyl-hexyloxy)-1,4-phenylene vinylene] (MEH-PPV) [56, 57], poly (9,9-dioctylfluorenyl-2,7-diyl) (PFO) [48, 58], and blended/multilayer polymers [59, 60] to give flexible and foldable LEDs. Furthermore, it is worthwhile to mention that the application of hybrid junctions of ZnO/polymer is not limited to LEDs but it is also used for many other applications such as solar cells [61] and sensors [62] as ZnO nanostructures provides an interesting alternative to all-organic counterparts. In fact, hybrid LEDs combine the advantage of both inorganic and organic semiconductors and they are perhaps superior to their all-organic counterparts in the sense that the active optical component in such hybrid structures is the inorganic nanostructure, which usually has a higher carrier mobility and lifetime than organic materials [63, 64]. Also, air stability of the inorganic materials is better than all-organic devices [65-68]. The emission spectrum of the hybrid LEDs covers

most of the visible range, giving rise to a white color impression. Even without further encapsulation, the device was shown to be stable over one hour under ambient conditions [65, 69].

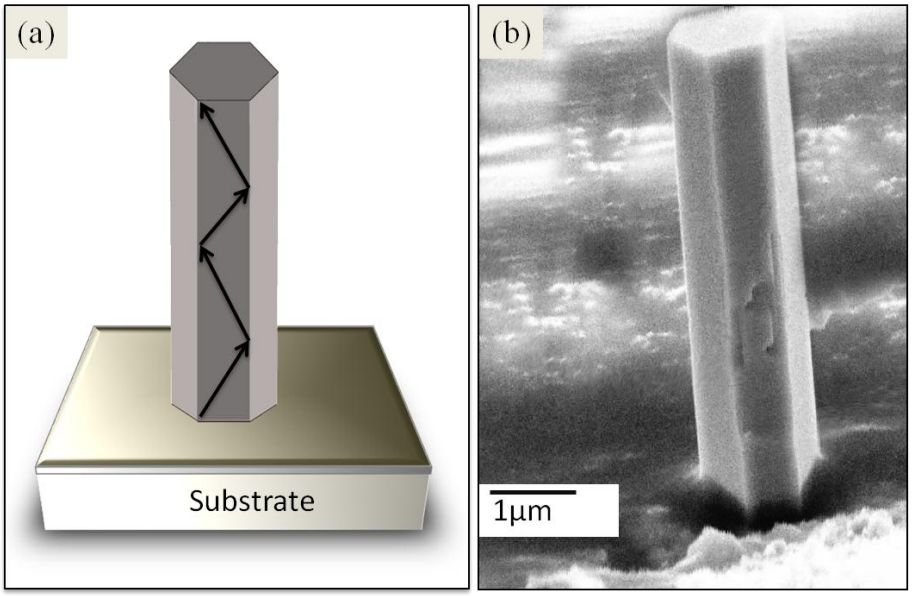

Figure 2.1: *(a) Schematic illustration of the working principle of ZnO nanorod in which photon is bouncing between (the two opposing facets), the two reflecting mirrors. (b) Shows cross-sectional SEM image of a ZnO nanorod.*

2.2 CuO based electrochemical sensors

The advancement of science and technology has created an overwhelming stream of opportunities for improving the quality of human life. In this context, metal oxide nanostructures with fascinating properties such as large surface area, chemical stability, electrochemical activity, being bio-safe and biocompatible combined with the ease of synthesis provide charming platform for interfacing biorecognition elements. Metal oxide semiconductors such as CuO nanostructures have attracted much interest because of its broad range of applications in electronics, sensors,

transducers, and biomedical sciences. These nanostructures also show high electron transfer kinetics and strong adsorption capability, providing suitable microenvironments for the immobilization of biomolecules and improved biosensing characteristics [1, 70]. CuO being relatively safe and biocompatible is one of the interesting and suitable oxide materials for biosensing applications. Electrochemical sensors are often simple and can offer real time analysis of analytes. Usually a sensor is composed of an analyte selective interface which is connected to a transducer that converts the observed physical/chemical change into measureable signal [32, 71-73]. The analyte selective interface can be membrane, protein or enzyme etc. and these interfaces are very much capable of recognizing, sensing, and regulating sensitivity and specificity with respect to the analyte [74]. Generally, biosensor can be classified into optical, piezoelectric, calorimetric and electrochemical sensor. Electrochemical sensors respond to electron transfer, electron consumption, or electron generation during a bio/chem.-interaction process. This class of sensors is of major importance and they are more flexible to miniaturization than other biosensors. Development of electrochemical sensors with high sensitivity, fast response time, and stability for the determination of different metal ions has been extensively explored [75, 76]. They are further divided into conductometric, potentiometric and amperometric devices. In potentiometric sensors the potential change due to the accumulation of charge on the working electrode is measured relative to the reference electrode when no current is flowing, whereas in amperometric sensors the current change due the electron transfer in the chemical reactions at the electrode at certain applied voltage. The working electrode potential is dependent on the concentration of the analyte in the solution while a reference electrode is needed to provide a specific reference potential. A biosensor is usually covered with a thin layer of enzyme or membrane for selectivity [77, 78]. Polymeric membrane is made of polymer, which can selectively transfer chemical species over other, and is a key component of potentiometric/amperometric ion sensors. Membranes are commercially available and routinely used for the selective detection of several metal ion such as Ca^{+}, Ag^{+}, K^{+}, etc [79].

2.3 ZnO/CuO heterostructures based humidity sensors

Humidity control and monitoring is important in diverse areas, such as paper and textile productions, food processing, hospitals, and libraries being among a few. In response to this situation various materials both as a resistive and capacitive humidity sensors have been investigated and developed [80]. Among others, ceramic resistive-type humidity sensors has received much attention, due to their easy preparation, high sensitivity, chemical thermal stability, reproducibility, low cost, long life and adherence to various substrates. For these humidity sensors, the changes in resistance are originating from the chemical reaction between the water vapor and the sample surface [81]. The ability of metal-oxide nanostructures to absorb water and hence change its dielectric properties gave rise to investigate the humidity sensors. The sensors made from metal oxides like iron oxide [82], TiO_2 [83, 84], aluminum oxide and tin oxide [85] have emerged as economic humidity sensors. Many researchers have reported ZnO [6, 86-89] and CuO [90] individually as a suitable ceramic material for resistive type humidity sensors. However, new materials, structures and intelligent mechanisms are always required in technology, as some time this becomes a key to overcome many challenges and problems. A new class of materials with promising applications to many areas, is that of hierarchically ordered nanohybrid metal oxides which exhibits structural ordering at multiple discrete length scale. Nanocomposite heterojuction sensors made by contacting *p*- and *n*-type oxide semiconductor (ceramic-ceramic interface) have attracted much attention since they were proposed by Nakamura et al. [91] for the detection of gases, because it is a system with intelligent sensing characteristics. Their behavior have stimulated many studies on CuO/ZnO system including humidity sensing [92, 93], but most of these heterojunctions have been assembled in a rather primitive manner, relying on pressing together the pellets to achieve mechanical contact between semiconducting disks. The act of mechanical pressing cause instability in the devices that limit their effective use as sensors because of the poor CuO/ZnO connectivity and low interfacial contact area, as demonstrated by Yu et al. [94, 95]. It is well-known that porous structures are attractive

for humidity sensors, water related conduction in such structures mainly occur as a surface mechanism [96], so the morphology and porosity could facilitate high sensitivity and selectivity to water molecule and good response time. Therefore it is interesting to synthesize nanostructures which not only have a high specific surface area but also distribute evenly and sparsely. Such structures would offer higher sensitivity towards humidity than a film-type, probably due to the larger capacity towards water adsorption. Recently, considering the importance of nanostructures and inspired by the advantages of high surface-to-volume ratios, fabrication of nanostructure based electronic devices and exploration of their properties became of great interest.

3 Materials Synthesis

This chapter describes the methods used in this work to synthesize nanostructured materials. Throughout this thesis, I have used the hydrothermal method to synthesis ZnO and CuO nanostructures. The focus and idea of this chapter is to mention important parameters affecting the growth in the hydrothermal method, which also set the condition for the choice of substrates for the development of devices, e.g. low operating temperature allows us to use polymer coated plastic and paper as substrates. This has led us to conduct several growth experiments under different conditions such as pH, temperature, precursor concentration, and time to rationally get control over the morphology of the nanostructures.

3.1 Substrate pre-treatment

The pre-treatment conditions of the substrate for the growth process, such as the pre-cleaning, concentration of the seed colloid, spin coating times, and annealing treatment of the substrate were the most important steps and had their respective influence on the morphology and quality of the ZnO nanostructures.

3.1.1 Substrate pre-cleaning

Prior to growth we immerse the substrate in iso-propanol and acetone in an ultrasonic bath each for 10 min and subsequently washed them with de-ionized water and then flushed them with nitrogen air. For Si substrate, one extra-step was required for removing the native oxide by immersing the substrate into diluted hydrofluoric acid (HF) solution (HF: water, 1:10) for 5 min, followed by washing in de-ionized water. Once the oxide layer was removed the grey color of the silicon surface visually appears.

3.1.2 Seed layer for ZnO nanostructures

One of the advantages of the hydrothermal method is the use of a seed layer prior to the growth in the form of nanoparticles or thin films.

This provides the nucleation sites for the growth of ZnO nanostructures. ZnO nanostructures can be grown on any hard or flexible substrate, such as Si, plastic, and paper.

Different solvents and precursors are being used for the preparation of the seed solution. We have chosen two different seed solutions in our work for making the seed layers. We prepared first the seed solution by dissolving 5 mM of zinc acetate dihydrate ($Zn(CH_3COO)_2$ $2H_2O$) in pure ethanol solution as previously reported by Green et al. [97]. We preferred the use of this seed for hard substrate because these substrates with spin coated seed layer need annealing at 250 ^oC for 30 min. to decompose $Zn(CH_3COO)_2$ $2H_2O$ into ZnO nanoparticles.

For the second case, we dissolved 5 mM of $Zn(CH_3COO)_2$. $2H_2O$ together with KOH in pure methanol solution prepared following the method developed by Pacholski et al. [98]. In this case annealing is not required for decomposition as it converts to ZnO nanoparticles at room temperature and is therefore very suitable for soft and flexible substrates. Atomic force microscope (AFM) image of the ZnO seed layer is shown in Figure 3.1.

In order to achieve ZnO nanostructures growth, we first spun coat (four times) the ZnO nucleation layer, at a speed of 3000 rpm for 30 seconds. During the growth, the ZnO nanostructures preferentially nucleate from the top of the nanoparticles grains. Tuning the spin speed enables the control of the density of nanoparticles on the substrate. In simple words, controlling the seed layer thickness or surface coverage can provide a good control of the alignment for the growth and density of the nanostructures.

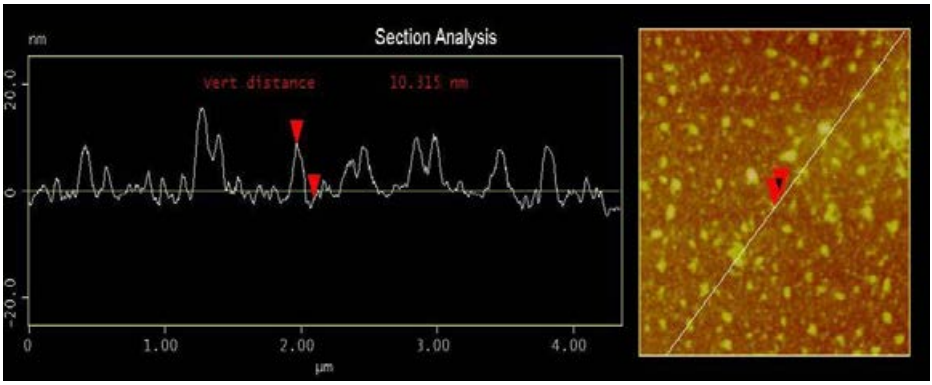

Figure 3.1 *AFM tapping mode image of the ZnO seed layer and the height profile (left) along the line [99].*

3.2 ZnO hydrothermal growth

There are several high and low temperatures ZnO and CuO nanostructures growth methods and both have some advantages and disadvantages. Comparatively hydrothermal methods are attractive due to many reasons. This method attained much interest in the scientific community when Vayssieres et al. [100] successfully demonstrated the growth of ZnO microstructures on a glass substrate. It does not require sophisticated equipment; it is low cost, environment friendly, and thus suitable for scale-up. Different morphologies of the nanostructures can be readily obtained by tuning the hydrothermal conditions [48, 101, 102]. In addition, the hydrothermal growth occurs at very low temperature and therefore holds great promise for nanostructures synthesis on a variety of flexible/soft plastic and paper substrates [103, 104]. The hydrothermal method has been demonstrated as a powerful and versatile method for synthesizing metal oxide nanostructures and so has been reported in the fabrication of electronic and sensing devices. The functioning of these devices is critically linked to the morphology of the nanostructures and hence requires tuning of the growth parameters for the optimal performance. In this thesis, we have synthesized ZnO nanorods [105], nanotubes [106, 107], flower-like [108], urchin-like nanostructures, CuO nanoflowers, and ZnO/CuO corals shape structures by the same method.

The schematic diagram of the hydrothermal growth procedure is shown in Figure 3.2.

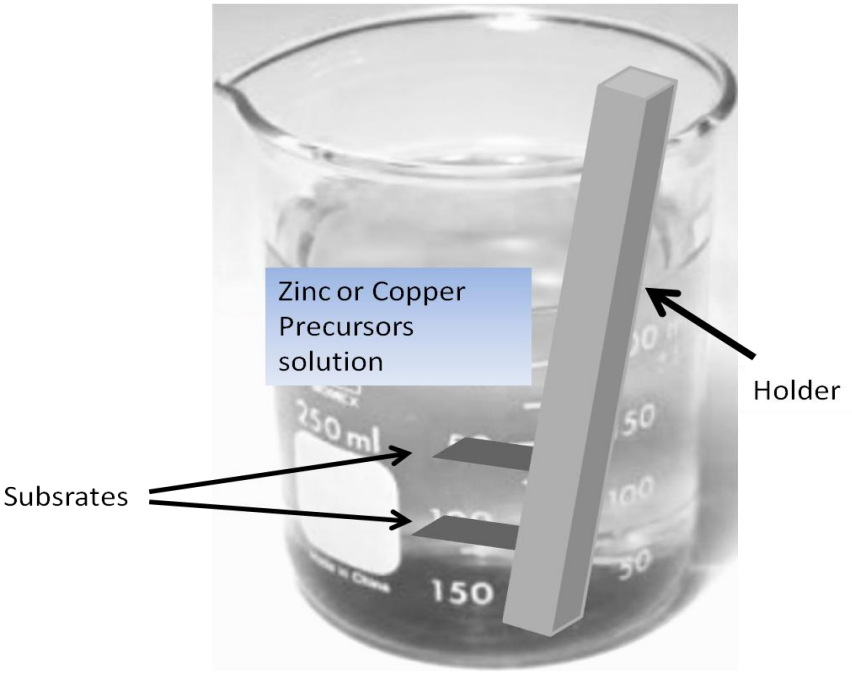

Figure 3.2: *Illustration of the hydrothermal growth method.*

3.2.1 Synthesis of ZnO nanorods

As long as the ZnO nanorods are concerned, the fabrication was carried out on different substrate such as Si, polymer coated plastic and paper substrates. Before finalizing the optimal conditions for ZnO nanorods growth on different substrate we have faced the problem of poor reproducibility, along with difficulty to control the size and the morphology. After systematic investigation, we used the following optimized conditions. The growth solution used in this method contained 100 mM of zinc nitrate hexahydrate ($Zn(NO_3)_2$. $6H_2O$) and 100 mM of Hexamethylenetetramine (HMT, $C_6H_{12}N_4$) while keeping their volume ratio at 1:1. We took the pre-seeded substrate and immersed it into a glass

beaker containing the nutrient solution; these were then kept for several hours in an ordinary laboratory oven at a temperature of 50- 90 °C for 4-5 h [105]. After the growth process, the samples were cleaned with de-ionized water several times, and dried in air. The possible mechanism of nanorods morphology elongated along one direction (c-axis) and shaped with a hexagonal cross-section can be explained from the wurtzite crystal structure of ZnO, which have a partial ionic nature [16]. The (001) plan in ZnO is polar and hence have the highest surface energy among the low index planes. As a result, the highest growth rate is along the [001] direction, and well oriented nanorods are easily formed in the c-axis orientation [16].

3.2.2 Synthesis of ZnO nanotubes

ZnO nanotubes have been fabricated by many approaches [13, 109] and are of particular interest for many application such as in high efficiency solar cell due to its higher internal surface area compared to nanorods, and yielding in brighter LEDs compared to nanorods [110]. We have fabricated nanotubes by etching process of the ZnO nanorods. We converted the ZnO nanorods into nanotubes by immersing the nanorods in KCl solution of concentration in the range of 3.0 to 3.4 M for time periods of 6 to 13 h, while the temperature of the solution was varied from 80 to 90 ^{o}C [7]. The immersion time was optimized by taking into account the nanorods dimensions in 3.4 M KCl solution at 85 ^{o}C resulting in 100% yield. The conversion ability of ZnO nanorods into nanotubes and the preferential etching process can be explained from polar and non polar surfaces of ZnO nanorods. The maximum energy (001) plane of ZnO nanorods results in the etching along the [001] direction since it decreases the system energy during the etching, and gradually leads to tabular morphology, while the non-polar planes with lower energy and stable planes are less favorable for preferential etching as illustrated in the schematic diagram of Figure 3.3 (a). Figure 3.3 (b-c) shows the ZnO nanorods (left) converted into ZnO nanotubes (right).

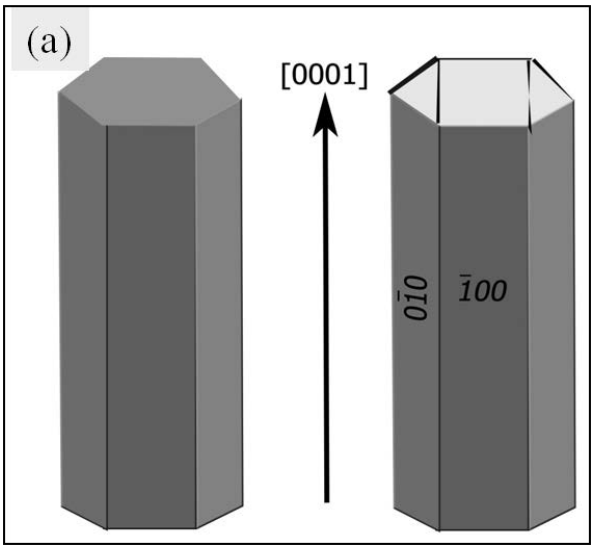

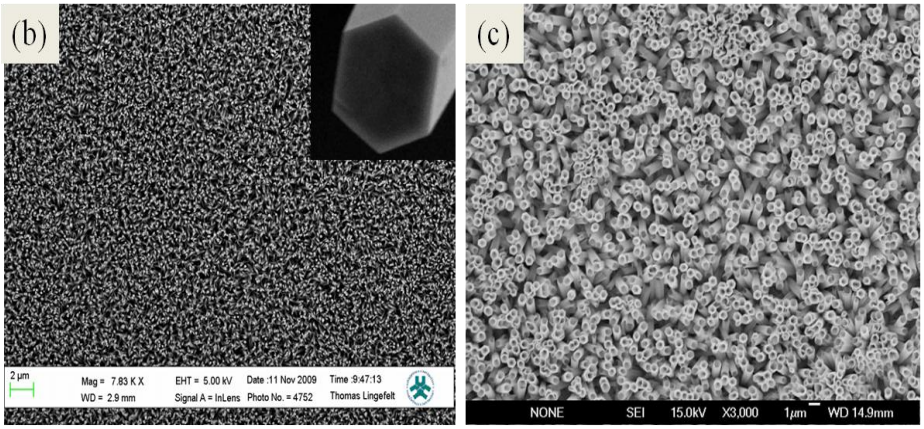

Figure 3.3 *(a) Schematic diagram of the ZnO nanorods and nanotubes growth behavior (b) show the SEM image of ZnO nanorods inset in an enlarge view of a nanorod showing clearly hexagonal shape, (scale 200 nm). (c) Scanning electron microscope image of the ZnO nanotubes.*

3.2.3 Synthesis of ZnO flowers-like /urchin-like structures

ZnO is an amphoteric material, i.e. it behaves as a base in acidic solutions and as an acid in alkaline solutions [15]. It is possible to synthesize ZnO in alkaline as well as in acidic environments. Previous finding shows that changing the pH of the growth solution can influence the preferred ZnO growth direction suggesting that such environment may provide a potential way of control over the ZnO nanostructures morphology. Expanding on these explorations, a rational approach to systematically alter the ZnO nanostructures morphology by means of adding bases or acids is developed. By introducing acid (HNO_3)/(HCl) or base ($NH_3.H_2O$)/(NaOH) we have been able to systematically control the solution's *pH* from 1.8 to 12.5 during the growth phase. Figure 3.4 shows the SEM image of ZnO nanostructures at different *pH* values.

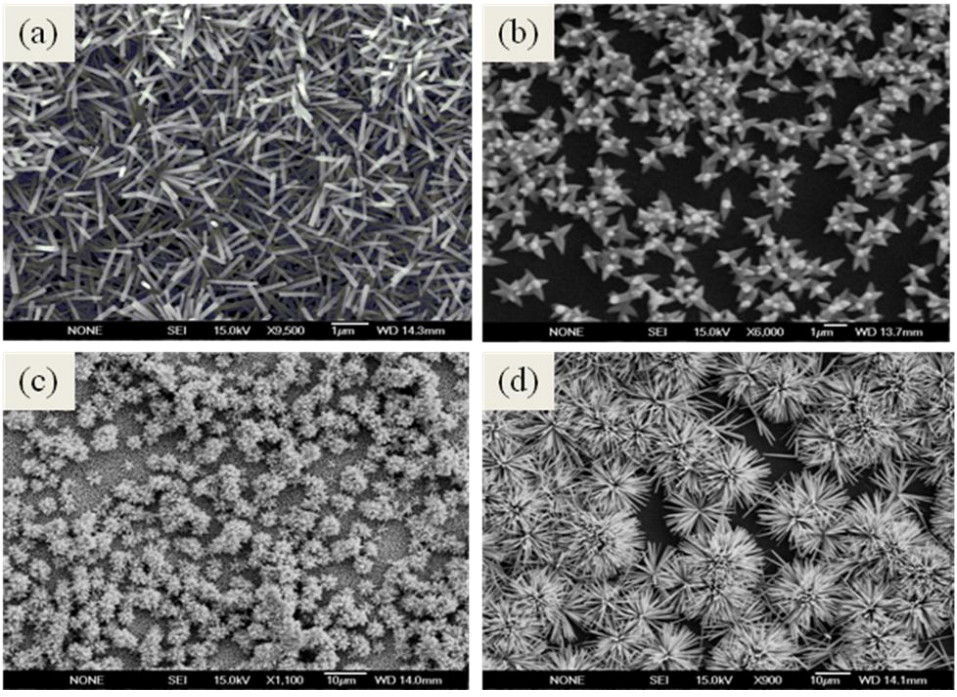

Figure 3.4: *SEM images of ZnO nanostructures; (a) nanorods on Si substrate at a neutral pH= 6.6, (b) Star-like nanostructures at pH =10, (c) flower-like nanostructures at pH =11, (d) Urchin-like nanostructures at pH =12[99].*

3.3 Synthesis of CuO nanostructures

3.3.1 Synthesis of CuO nanopetals

Petal-shaped CuO nanostructures composed of triangular shaped leaves were synthesized by the hydrothermal method as shown in the SEM image of Figure 3.5 (a). In the typical experimental procedure, 5 mM of copper nitrate and 1 mM of HMT were dissolved in 100 ml of de-ionized (DI) water under constant stirring. The obtained bluish solution was formed due the presence of copper ions. The solution was transferred into a glass beaker and was loaded together with a substrate into a laboratory oven at 90 ^{o}C for 4 to 5 h. After the growth, the vessel was naturally cooled and a resulting black product of CuO nanopetals was collected and washed several times with DI water.

3.3.2 Synthesis of ZnO/CuO nanocorals

Nanocorals of CuO/ZnO were grown by a hydrothermal growth method as illustrated in Figure 3.5 b-d. Two steps were applied to ensemble the nanocorals growth; lengthwise growth, and branched growth. Lengthwise growth of the ZnO nanorods in the first generation was performed by the method in [111]. For the branched growth process of CuO nanostructures, freshly grown nanorods substrate was submerged having face up in a 5 mM aqueous solution of [$Cu(NO_3)_2.3H_2O$], and then heated to 60 ^{o}C for 1.5-4 h. The branched growth produced highly branched CuO nanopetals by selectively growing on the column structures of ZnO nanorods. It is also clearly evident from the SEM images (Figure 3.5 b-d) that the CuO branch growth densely and selectively decorated each individual nanorod. However, changing the above mentioned conditions or adding surfactants the growth of CuO nanostructures still occur but they where no more selectively attached to the ZnO nanorods instead they were precipitated on the ZnO nanorods surface.

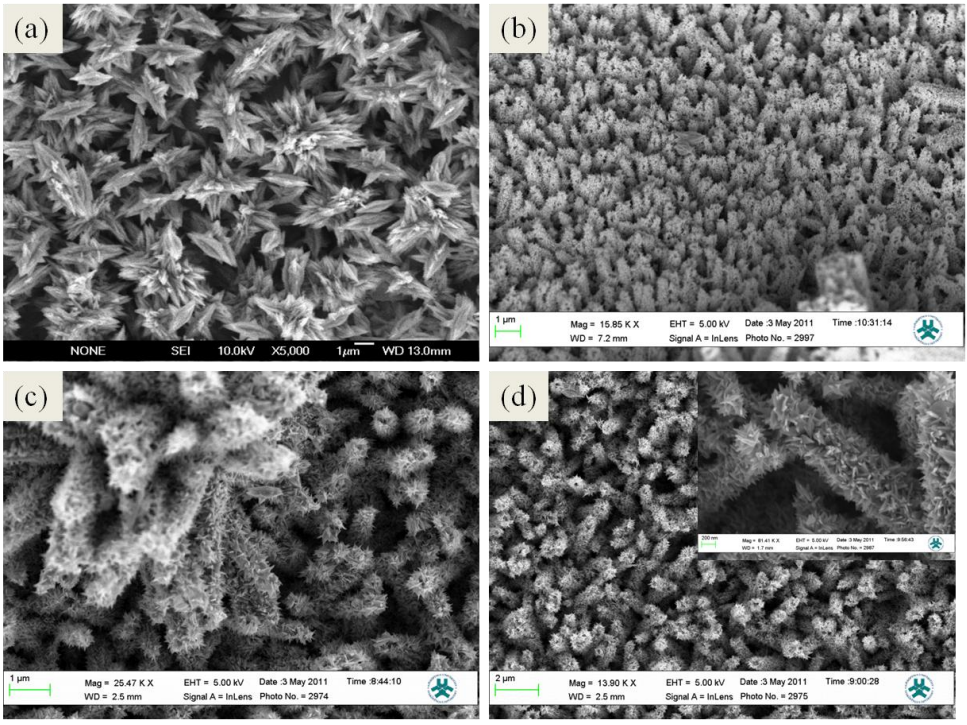

Figure 3.5: *SEM images of (a) CuO nanostructures, (b) ZnO/CuO nanocorals (c)-(d) ZnO/CuO nanocorals and the inset in (d) is the magnified view of the nanocorals.*

Here at the end of the nanomaterials synthesis chapter it is good to mention visible color appearance of the samples. Optical photograph images of grown materials are shown in Figure 3.6 displaying different visible colors of the surfaces. ZnO is whitish in color so it is obvious that on gold coated surface it appears golden while on Si substrate it appears whitish blue in color. Similarly, CuO samples surface appear black in color, while ZnO/CuO also appeared black due to CuO on the top of the ZnO.

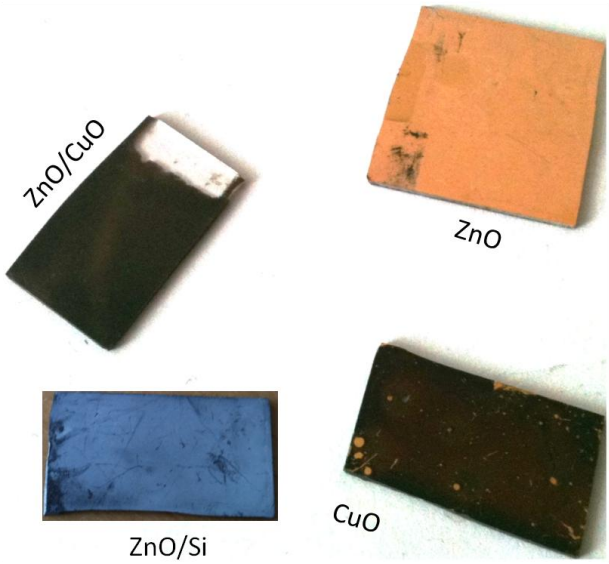

Figure 3.6: *Photograph images show the visible observation of different grown nanomaterials samples, such as ZnO, CuO, and nanohybrid ZnO/CuO structures grown by the hydrothermal method.*

4 Fabrication of Devices

The ability of ZnO and CuO to be engineered into interesting nanostructures, as discussed in the previous chapter and it gives them great potential for use in a wide number of future applications. In the present chapter we will deal with some applications of those nanostructures.

In the first part of the chapter, ZnO/polymer hybrid LEDs characteristics will be explained. As mentioned in the previous chapter ZnO has several advantages over its competitors, namely GaN; it is inexpensive, relatively abundant, chemically stable, easy to synthesize/process and non-hazardous. In my work I have used ZnO as an active component for optoelectronic devices, but the new applications of ZnO in electronics are much broader than that.

In the later half we will deal with CuO and ZnO/CuO nanostructures utilized as sensors. Flower-like CuO nanostructures were reported to have very high sensitive performance to H_2O_2 [8], and many other gases [112, 113]. We have utilized CuO petal-like structures for Ag^+ detection. With the aim to increase the sensitivity of humidity sensors, the unique ZnO/CuO hierarchical structures were used as bifunctional material for humidity sensing. The procedure for sensing devices will be discussed in the chapter.

4.1 ZnO-based devices

The following section briefly describes the preparation of hybrid ZnO/polymer LEDs.

4.1.1 Hybrid ZnO/polymer heterojuction LEDs by solution-based method

An ordinary clean room paper is used as substrate for ZnO nanorods-polymer hybrid LEDs and the schematic diagram of LED is shown in the Figure 4.1 (a). Usually paper has an insulating and rough surface and it can degrade in water and other nutrient solutions. In order to overcome these difficulties we have modified the surface of the paper substrate by spin coating a cyclotene layer (BCB 4022-35 Dow Chemical's), followed by

vacuum baking at 110 °C for 1 hour. The cyclotene barrier layer, not only protects the surface of the paper from the nutrient solutions and water during processing, but it also reduces the surface roughness. After that we filtered the poly (3,4-ethylenedioxythiophene) poly(styrenesulfonate) (PEDOT:PSS) solution with 0.45 μm pore size filter, which was then spin coated on the entire substrate at a speed of 2000 rpm, followed by baking at 70 °C for 2 hour. We covered some area to be used for bottom contacts and then we spin coated the PFO (American dye source ADS 129 BE) conducting blue emitting polymer layer at a speed of 2000 rpm, followed by baking at 70 °C for 10-15 minutes. In order to achieve ZnO nanorods growth we used the same methods mention in the chapter 3.

In order to process the samples for devices we spun coated a polymethyl methacrylate (PMMA) layer, to electrically isolate neighboring nanorods from each other, at a speed of 3000 rpm for 30 seconds and then baked it at 90 °C for 1 min. Reactive ion etching (RIE) was used to etch the PMMA layer to expose the tips of the nanorods [12]. SEM image of spin coated PMMA layer is shown in Figure 4.1 (b). The image clearly indicates that spin coating process of the insulating layer fills the gap between the nanorods and insulate them from each other. The surface of nanorods covered with PMMA is etched away after exposing to oxygen in the RIE. We then evaporated 50 nm aluminum (Al) top contacts while the bottom contact to the PEDOT: PSS was achieved by applying silver (Ag) paste. SEM image of a fabricated device is shown in Figure 4.1 (c).

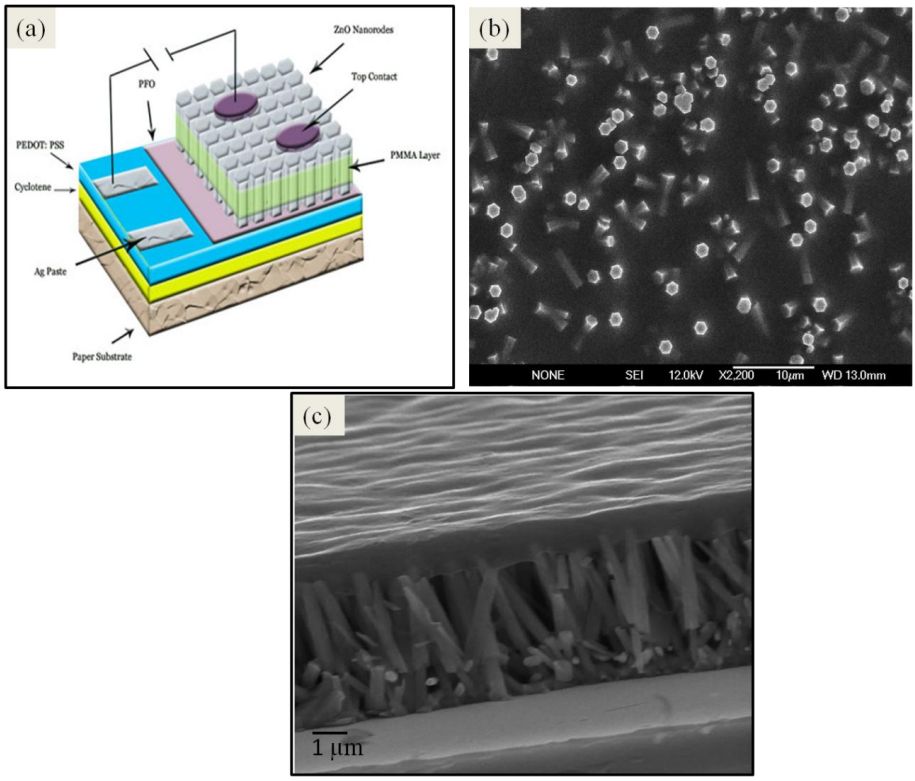

Figure 4.1: *(a) Schematic illustration of the working principle of ZnO nanorods/polymer LED. (b) SEM Image of the ZnO nanorods with insulating layer (before top contact deposition) (c) SEM image of the ZnO nanorods LED device grown on glass substrate [114].*

4.1.2 Printed ZnO /polymer heterojuction LEDs

To fabricate printed ZnO/polymer LEDs, we have investigated different organic dispersant for ZnO nanorods to get a potentially printable ink. After finalizing the organic dispersant, specified amount of ZnO nanorods was dispersed in the organic dispersant, yielding a printable ink. A layer of this ink was printed on the patterned substrate layer (Figure 4.2 (a-b). The patterned layers were prepared as follows. First, we printed a pattern of PEDOT: PSS on paper/plastic substrate and then a PFO layer was spin coated using spin speed of 2000 rpm for 30 seconds either on paper or plastic substrate (Figure 4.2 (b-d). For printing the ZnO nanorods

a screen printing paste was manufactured by dispersing ZnO nanorods (5.2 g) in a solvent based screen printing varnish, Plastijet XG 383 (2.5 g, 50%), manufactured by Fujifilm Sericol Ltd, and a small amount (1.1 g) of a retarder, Plastijet ZV 558, was added. The mixture was stirred using an Ultra Turrax™ Tube dispenser before printing. Screen printing was performed using a nylon web 120-34 (wires per inch and wire diameter in mils) for both electrodes and ZnO nanorods paste, using a semiautomatic flat-bed screen printing machine, Screen-printer TIC SCF 550, Eickmeyer. The printed substrates were dried at 90 ^{o}C in an oven after printing. Finally, we applied aluminum contacts and proceeded for the measurements. Electroluminescence (EL) spectra were acquired on an Andor Shamrock 303iB spectrometer supported with Andor-Newton DU-790 N CCD.

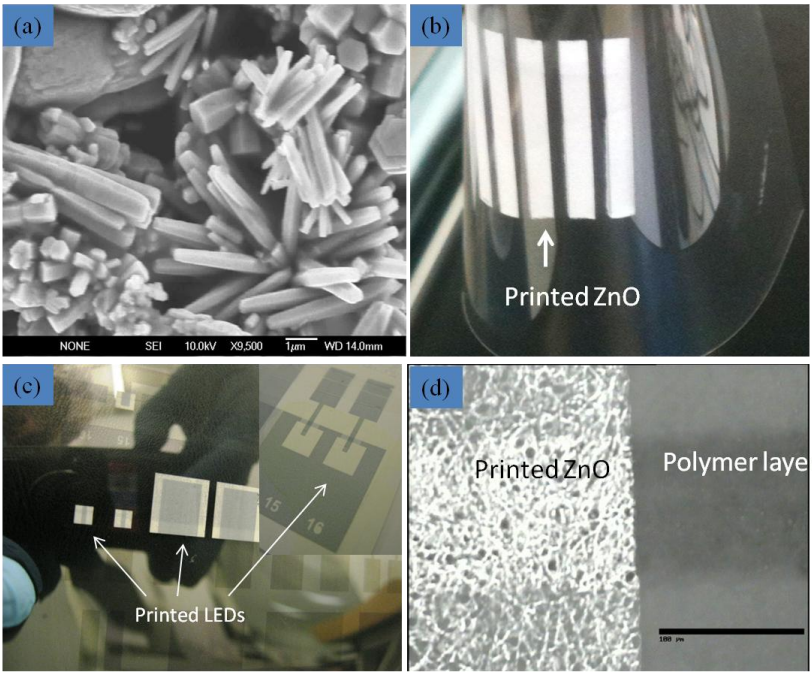

Figure 4.2: *(a) SEM image of the hydrothermally grown ZnO nanorods in powder (b) Photograph image of the printed ZnO nanorods (c)shows the photograph of the printed ZnO/polymer LED device on plastic substrate, where inset show the same device on paper substrate (d) Optical image of the printed ZnO nanorods layer [115].*

4.2 CuO-based devices

The following section provides a brief description of the fabrication of the electrode that was used as an electrochemical and humidity sensor.

4.2.1 CuO-based electrode fabrication

CuO nanopetals (NPs) were initially grown on gold coated glass substrate by the method mentioned in the previous chapter. To prepare the selective electrode and make the CuO surface highly selective for Ag^{+}, a polymeric membrane containing ionophor-IV was used. In brief, 64 mg of powdered PVC was dissolved in 6 mL of tetrahydrofuran (THF) together with 112 mg of a plasticizer DBP, 8 mg of a NaTPB and 6 mg of Ag^{+} selective ionophore-IV. The resulting solution was rigorously stirred until all the reactants were dissolved. The CuO NPs surface was coated with the membrane by drop coating procedure. For functionalization, the prepared electrodes were allowed to dry at room temperature. Finally for conditioning the working electrode for Ag^{+} selectivity, the samples were soaked into 100 mM Ag (NO_3) solution for 15 min. Electrical connections were applied using highly conductive silver paste.

4.2.2 ZnO/CuO nanohybrid humidity sensor fabrication

The materials investigated here were copper (II) oxide and zinc oxide. These materials were chosen for their ease of synthesis using the hydrothermal method and their relative abundance. They have an added benefit of being natural *n* and *p* type materials. Un-doped zinc oxide has intrinsic n-type conductivity, and CuO is naturally p-type. In order to get two electrode configurations, a gold and indium tin oxide (ITO) thin films were used for the top and the bottom contacts, but future work will include investigations using more economical alternatives. The process of growing the structures and their benefits has been discussed in the previous chapters.

5 Characterization Techniques

The first step towards being able to correlate the function of a certain material in a device is to have in-depth knowledge of the material structure and its morphology. In this chapter characterization techniques used for the structural study of the ZnO and CuO nanostructures are introduced with some detail of the electrical, electro optical measurements of LEDs and electrochemical sensor devices. The governing principle of each technique is introduced followed by experimental results with explanation in the discussion part.

5.1 Structural characterization techniques

5.1.1 Scanning electron microscopy (SEM)

Scanning electron microscopy (SEM) is widely used within different scientific fields for the characterization of nanomaterials, nanostructures, and is an excellent technique for investigating the surface morphology at the nanoscale dimensions. By using SEM it is often possible to distinguish features on the scale of 10 nm or less [116]. Imaging of nanostructures materials using SEM mostly does not require complex sample preparation (the sample needs only to be conductive and vacuum compatible). The basic working principle of SEM [117] is shown in the schematic diagram of Figure 5.1. The SEM uses electrons instead of light to generate an image, an electron beam is focused and scanned over a selected area of the surface of the sample under investigation, hence the name scanning electron microscope. In an SEM, when an electron beam strikes a sample, a large number of signals are generated. Depending on the type of detector, the detected signal is converted to an image of sample's surface topography or to investigate its composition. I have used SEM to investigate the morphology and dimensions of the ZnO and CuO nanostructures. For this purpose, secondary electron detector is used. Secondary electrons have typical energy of 3-5 eV, they can only escape, depending on the accelerating voltage and surface density of specimen, from nanometers depth of materials surface. Secondary electrons are principally used for the visualization of surface texture/morphology and

roughness, as they accurately mark the position of the beam on the sample surface and give topographic information with high resolution.

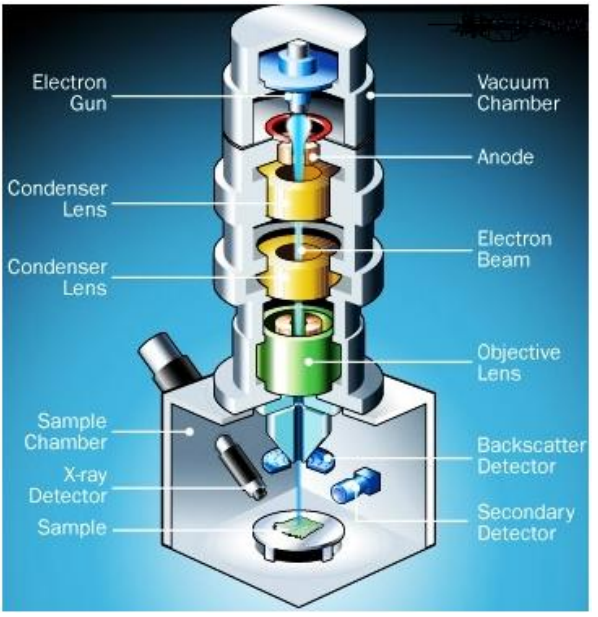

Figure 5.1: *Schematic diagram of a scanning electron microscope [118].*

Figure 5.2 (a-f) show some SEM images of various morphologies of ZnO nanostructures that have been synthesized under different hydrothermal conditions where (g) shows the SEM image of CuO nanostructures and (h) shows the nanohybrid nanostructures of ZnO/CuO which were also synthesized by hydrothermal route under different conditions.

Together with other characterization techniques, this gives us information about the morphology, dimensions and crystallinity of the nanostructures.

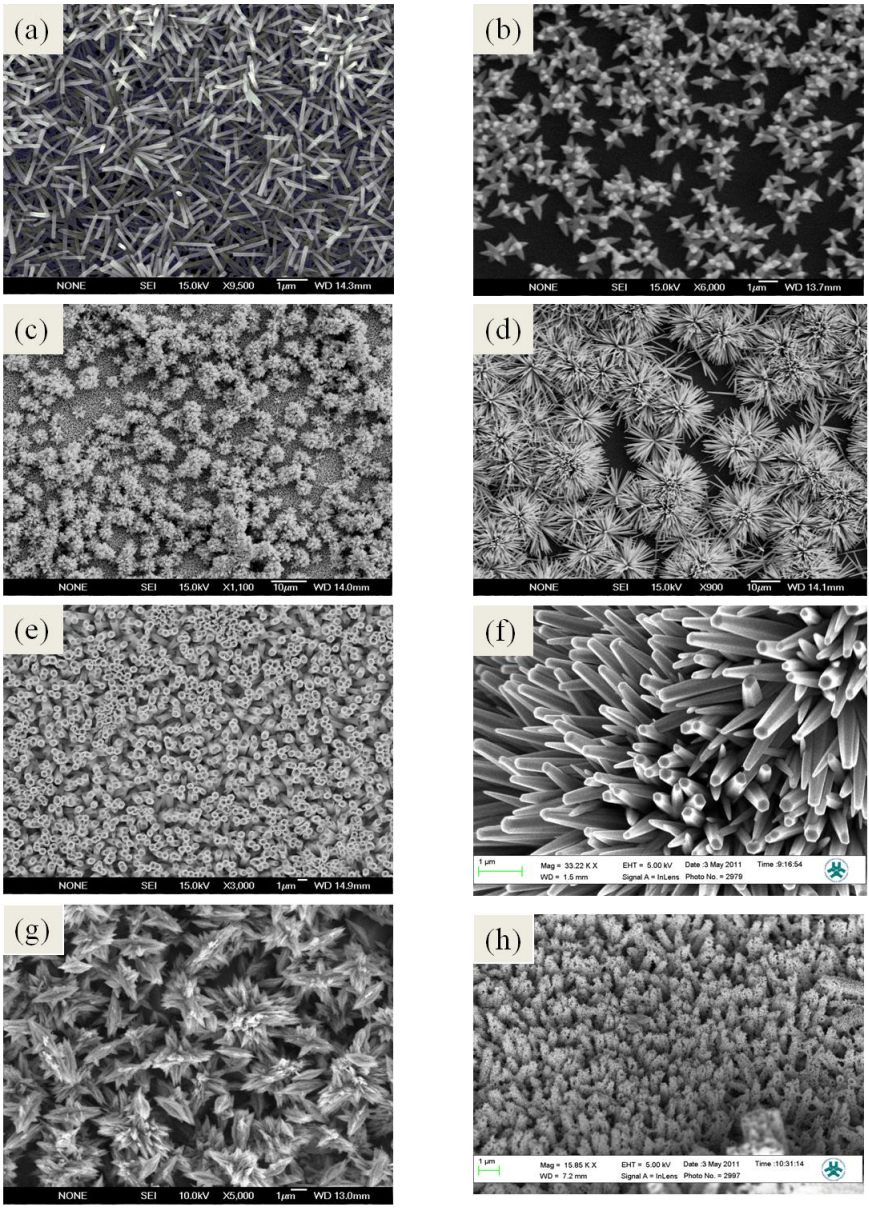

Figure 5.2: *SEM images of ZnO nanostructures; (a) nanorods on Si substrate at neutral pH= 6.6, (b) star-like nanostructures at pH =10, (c) flower-like nanostructures at pH =11, (d) urchin-like nanostructures at pH =12, (e) nanotubes grown on Si substrate, (f) nanorods grown on a paper substrate. (g) shows the SEM image of CuO nanostructures and (h) shows the nanohybrid structures of ZnO/CuO [99].*

5.1.2 Transmission electron microscopy (TEM)

Transmission electron microscopy (TEM), like SEM, belongs to the group of electron microscopes. The basic principle of a TEM is similar to that of an optical microscope with a replacement of light with high energy electrons source (200 keV) and glass lenses with magnetic lenses. TEM is a valuable instrument for characterizing materials as it can provide few angstroms resolution imaging as well as crystallographic and chemical information depending on the mode of operation. Atomic scale resolution can be obtained by the Rayleigh criterion; the smallest distance resolved being directly proportional to the wavelength of the radiation used. Thus, high energy electrons with de Broglie wavelengths in the sub-angstrom range provide atomic resolution. The basic working principle of a TEM is shown in the schematic diagram of Figure 5.3. Unlike SEM, sample preparation is tedious in TEM imaging. The reason for this is the fact that the electron beam passes through the sample meaning that the sample has to be electron transparent, i.e., very thin. To achieve this, in some cases the samples must be carefully prepared using polishing and etching, however, I have prepared the samples by dispersing the nanostructure in ethanol and drop casted on the copper grid which is relatively easy method. When the electron beam used in the TEM passes through the sample under study, the electron beam interacts with the sample, which causes the electrons to scatter. The amount of unscattered electrons that pass through a certain part of the sample depends on the scattering potential and thickness of that specific part of the sample. These unscattered electrons are collected by a detector and provide the contrast in the image of the sample, where the variation in darkness is determined by the variation in density. Looking at the scattered electrons, diffraction patterns can be obtained, which gives information about the crystal structure of the sample. Transmission electron microscopy has been used for material characterization in some of the papers included in this thesis.

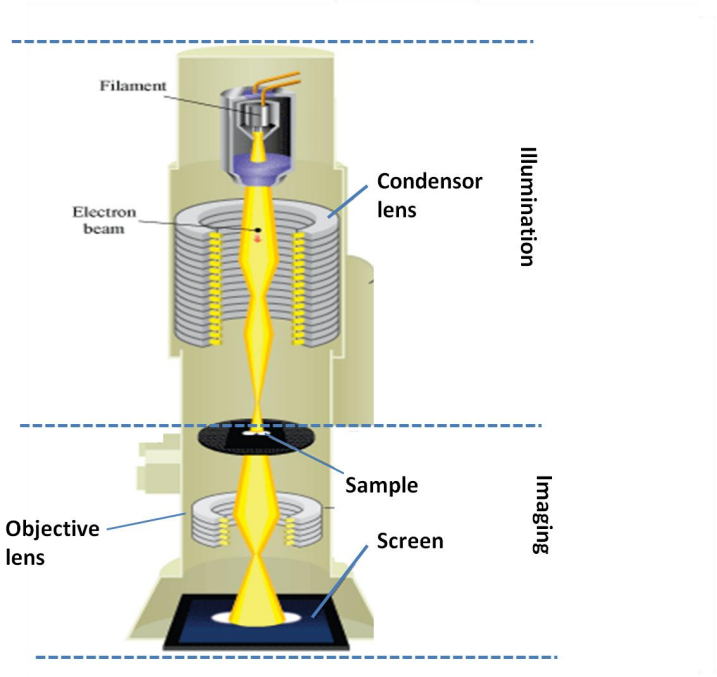

Figure 5. 3: *Schematic diagram of a TEM. Generally TEM is divided into two main parts: illumination and imaging system [119].*

An individual single ZnO nanorod was characterized using the TEM (Figure 5.4). The image illustrates that the ZnO nanorod has a high quality single crystal structure and follows [001] growth direction (inset of Figure 5.4-right). The corresponding selected area electron diffraction (SAED) further proves the single crystalline nature of ZnO nanorod and their [002] growth direction (inset of Figure 5.4-left).The cluster morphology was observed in the growth which is also shown in the image and suggests that multiple nanorods often grow from other nanorods in solution methods.

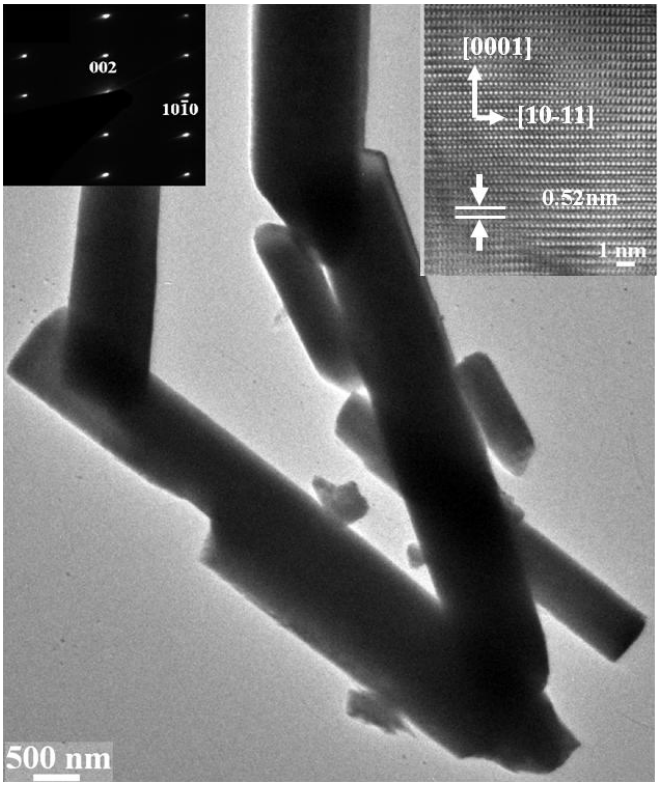

Figure 5.4: *TEM image of the ZnO nanorods, inset (right) show HRTEM image of the individual nanorods while inset (left) shows the corresponding SAED pattern [115].*

The morphology and crystallographic structure of the as-grown CuO nanopetals was also analyzed by high resolution transmission electron microscopy (HRTEM), and selected area electron diffraction (SAED). A bright field TEM image of CuO nanopetals in Figure 5.5 shows that the length and width of the CuO nanopetals are in the range of 2-3μm and 1-1.2 μm, respectively. The images exhibit that a CuO nanopetals contains a bright single area together with some dark domains at the centre. The bright area is the main part, while the dark domains are the side parts which grow interpenetrating with the main part. The main part and side parts have a twin relationship between each other. The twin relationship is

(101)[010]//(101)[010] twin. The combined analysis of the HRTEM images and the SAED pattern reveals that each part is single crystalline but all parts preferentially grow along the co-axis [010] direction with (001) as their surface as shown by figure 5.5 (b, c).

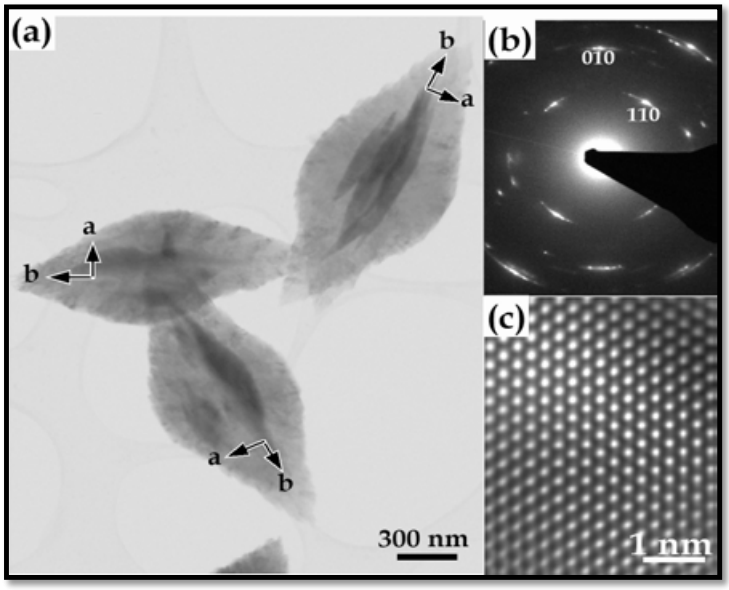

Figure 5.5: *(a) TEM images of the as grown CuO nanopetals. (b) Associated SAED pattern (c) HRTEM image of the specified area.*

5.1.3 Atomic force microscopy (AFM)

Atomic force microscopy (AFM) is a non destructive and very high-resolution imaging technique, with demonstrated resolution in the order of fractions of a nanometer. The AFM is one of the most widely used tools for imaging, measuring, and manipulating samples at the nanoscale. There is no special sample preparation required in this technique and the measurements can be carried out at ambient environment. Figure 5.6 illustrate the block diagram of AFM. In AFM the information is gathered by "feeling" the surface with a mechanical probe. Piezoelectric scanners that facilitate tiny but accurate and precise movements on command enable very precise scanning. The AFM consists of a cantilever with a sharp tip (probe) at its end is used to scan the specimen surface. When the tip is

brought into proximity of a sample surface, forces between the tip and the sample lead to a deflection of the cantilever according to Hooke's law. Typically, the deflection is measured using a laser spot reflected from the top surface of the cantilever into an array of photodiodes. If the tip was scanned at a constant height, a risk would exist that the tip collides with the surface, causing damage. Hence, in most cases a feedback mechanism is employed to adjust the tip-to-sample distance to maintain a constant force between the tip and the sample. Traditionally, the sample is mounted on a piezoelectric tube, which can move the sample in the z direction for maintaining a constant force, and the x and y directions for scanning the sample. The resulting map of the area z = f(x, y) represents the topography of the sample [120, 121].

Figure 5. 7: shows the 3 µm x 3 µm AFM image of ZnO seed layer. From this AFM image, it can be revealed that the height of ZnO nanoparticles on the substrates is about 20 nm and the dispersion of ZnO nanoparticles is also visible and those particle act as nuclei for ZnO nanostructures growth.

Figure 5. 8: shows the AFM image of ZnO nanorods. It shows that dense nanorods are grown uniformly on the substrate having diameter of about 150 nm.

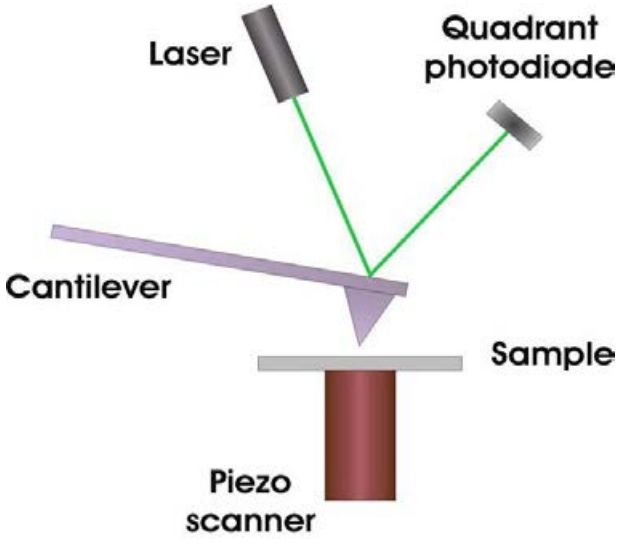

Figure 5. 6: *Shows the block diagram of Atomic Force Microscope [122].*

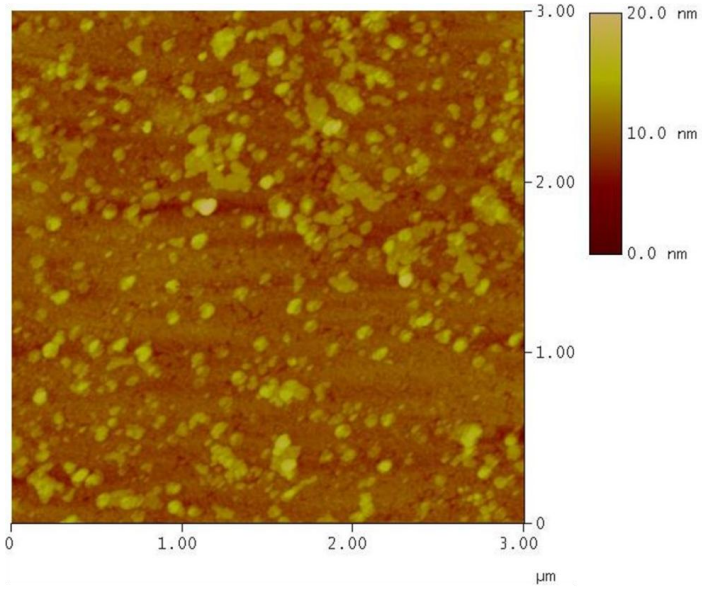

Figure 5. 7: *The 3 µm* x *3 µm AFM image of the ZnO seed layer.*

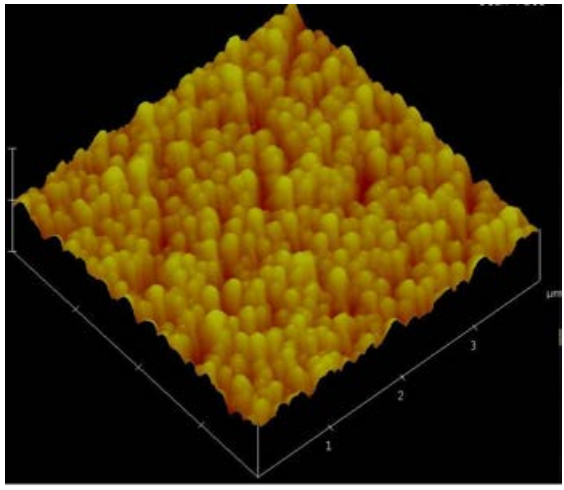

Figure 5. 8: *AFM topographic image (4 µm x 4 µm) of ZnO nanorods recorded in tapping mode by Digital Instruments Nanoscope AFM system.*

5.1.4 X- ray diffraction (XRD)

X-ray diffraction is a powerful tool to study the crystal structure of semiconductors. XRD gives information about crystalline phase, quality, orientation, composition, lattice parameters, defects, stress, and strain of samples. Every crystalline solid has its unique characteristic X-ray diffraction pattern, which is identified by this unique ‘‘fingerprint’’. Crystals are regular arrays of atoms and they are arranged in a way that a series of parallel planes separated from one another by a distance *d*. Figure 5.9 shows the detail of the process of x-ray diffraction. If an x-ray beam with a wavelength λ strikes the sample with an incident angle θ then the scattered ray is determined by Bragg’s law:

$$n\lambda = 2d\sin\theta$$

Where n is an integer, λ is the wavelength of the beam, d is the spacing between diffracting planes, and θ is the incident angle of the beam. The set of *d*-spacing in a typical x-ray scan provides a unique characteristic of the samples in question.

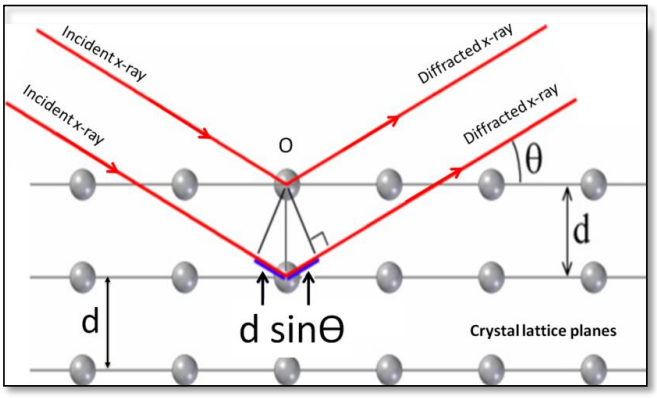

Figure 5. 9: *Schematic diagram of Bragg's reflection from lattice planes in a crystalline structure.*

X-rays diffraction measurement has been performed with a diffractometer (X'pert PANalytical) equipped with Cu Kα1 (λ=1.5406 nm) using a generator voltage of 40 kV and a current of 40 mA.

Figure 5.10 shows XRD pattern of ZnO nanorods grown on Si substrate. The observed diffraction peaks in the recorded XRD pattern agrees well with the values available in the JCPDS card 36-1451for hexagonal ZnO with wurtzite structure. The relative intensity of the (002) peak appeared high as expected for the case of aligned ZnO NRs grown on a substrate [105]. No characteristics peaks of other impurities were observed in XRD pattern, indicating that phase-pure and high quality ZnO nanomaterials are readily obtained. Figure 5.11 shows the XRD curve of CuO nanopetals where the diffraction peaks can be readily indexed to CuO (JCPDS 05-0661). The XRD pattern demonstrate the presence of a single tenorite phase of CuO with no indication of Cu_2O and $Cu(OH)_2$ phase [123]. The CuO XRD scan has fewer counts and is noisy when compared to the ZnO XRD scan.

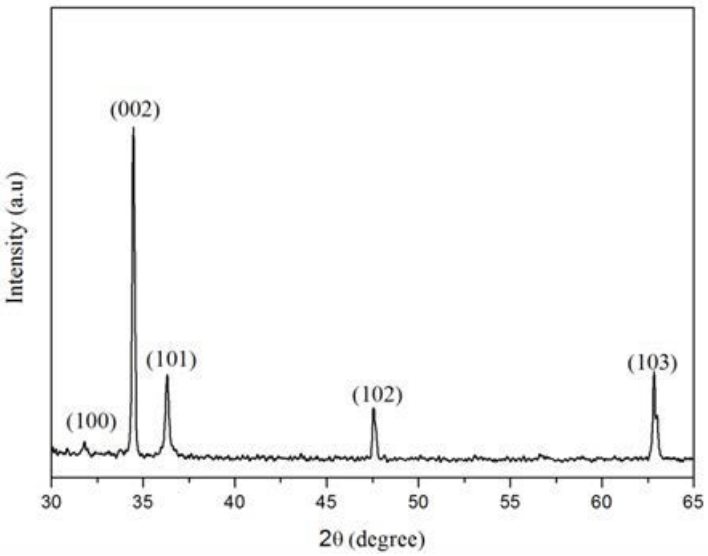

Figure 5.10: *XRD pattern of ZnO NSs grown at T = 90 ^oC, for duration t = 5 h and at inherent pH.*

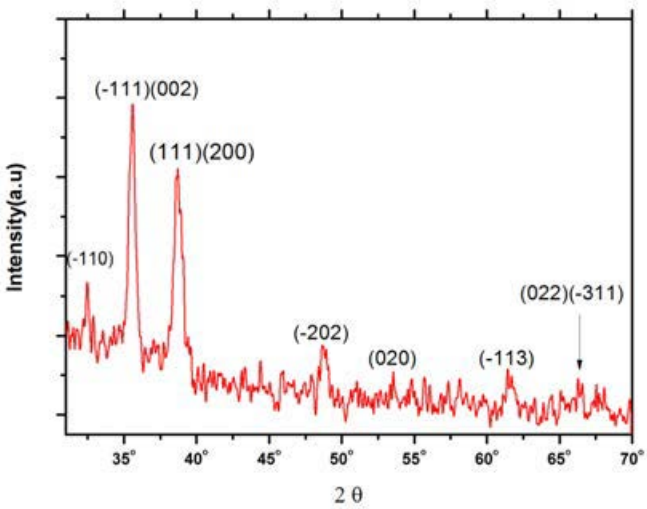

Figure 5.11: *XRD pattern of the as-grown CuO nanopetals by the hydrothermal method.*

Figure.5.12 is an XRD scan of a ZnO/CuO nanohybrid structure. The phase separation between ZnO and CuO is visible confirming the existence of both ZnO and CuO. ZnO peak intensities occur at 2θ values of 31.8^{o}, 34.4^{o} and 36.3^{o}, while those for CuO occur at 2θ values of 35.5^{o} and 38.78^{o} [105].

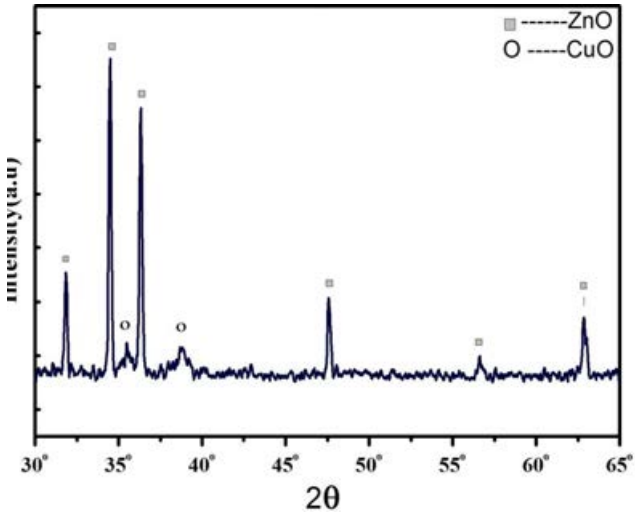

Figure 5.12: *XRD pattern of ZnO/CuO nanohybrid structures grown by hydrothermal method.*

5.2 Electrical measurement

5.2.1 Current-voltage (*I-V*) characteristic

Current–voltage (*I-V*) characteristic of *p-n* junctions give the key information to judge the performance/quality of the fabricated diodes. *I-V* measurements were performed for the fabricated diodes/LEDs by using a multiple source-measure units (SMUs) semiconductor parameter analyzer (PA) Agilent 4155B. Two SMU terminals are connected through the coaxial cables and micromanipulators to the cathode and the anode. The current response is measured when the voltage is swept in a constant interval. From the *I-V* characteristics different information can be extracted about the device such as the turn-on voltage, ideality factor, break-down voltage, and parallel and series resistance of the fabricated device [124-126]. By forward biasing the diode, the internal electric field will decrease and the majority charge carriers will diffuse into the depletion region reaching flat band conditions, i.e. compensation of the band bending, and even higher voltage, the current increases exponentially until the current start to be limited by the series resistivity of the diode.

Figure 5.13 shows the resulting Au/ZnO nanotubes (NTs) heterojuction exhibiting good rectifying *I-V* characteristics. Such type of rectification behavior is best described by the thermionic emission theory. According to this theory, the current in such a device could be expressed as:

$$I = I_S\left[\exp\left(\frac{qV}{nkT}\right)-1\right]$$

where I_s is the saturation current, k is Boltzmann constant, T is the absolute temperature, q is the elementary electric charge, V is the applied voltage, and n is the ideality factor. The saturation current I_s is given as:

$$I_S = AA^*T^2\exp\left(-\frac{q\Phi_b}{kT}\right)$$

where A is the active device area, A^* is the effective Richardson constant and Φ_b is the barrier height. In Paper 3, detailed *I-V* analysis of the diodes manufactured on ZnO nanotubes is discussed.

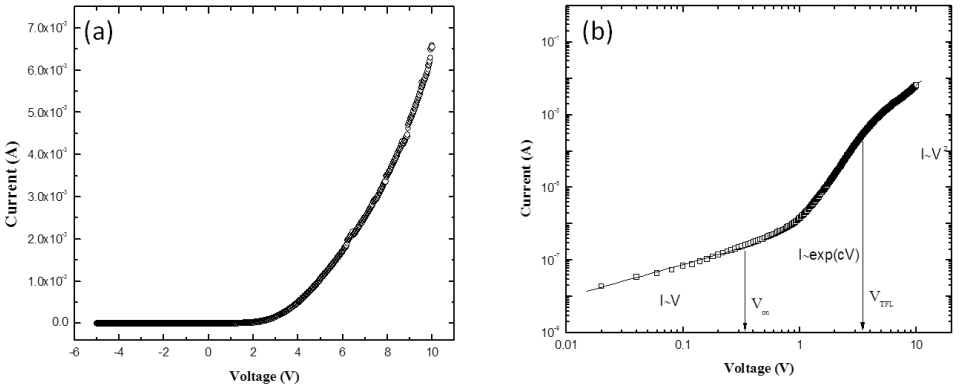

Figure 5.13: *Typical current-voltage (I-V) characteristics of Au/ZnO NTs Schottky diode. (b) Log-log plot for the I-V data of Au/ZnO NTs Schottky diode [127].*

5.2.2 Electrochemical measurements using CuO nanostructures based sensors

Electrochemical measurement was carried out using two electrode configurations of CuO nanopetals as the working electrode and an Ag/AgCl as a reference electrode. The electrochemical response was measured using a source meter Keithley 2400 at room temperature. Figure 5.14 shows the schematic diagram of the measurement set-up. The electrochemical response was observed until the equilibrium potential reached the stabilization point and then the electrochemical potential was measured [128].

Figure 5.15 (a) shows the stability and output response curve of the fabricated CuO nanopetals working electrode. The output response of the fabricated electrochemical sensor showed good stability for around 20 sec

which shows the fast electrochemical reaction between CuO nanopetals and Ag^+. We checked the selectivity and stability of the sensor by adding some interfering ions to 1 mM $AgNO_3$ solution and observed the effect on the output response curve, with interfering ions (blue and red) and without (black) interfering ions. The blue curve shows that as soon as we introduced the interfering ions such as Cu_2^+, Co_2^+, K^+, Cs^+ etc. with same molar concentration, we found disturbance in the stability for a short time, but the signal retained back to stable form. If we, however, introduced interfering ions at considerably much higher concentration than that of the Ag^+, the sensor signal was clearly affected (red curve). It could be because of the unique electro catalytic behavior of CuO nanostructure which combines with high characteristics of electrochemistry (fast, sensitive, selective and low detection limit). It is expected that bio-chemical species are covalently attached to the surface of metal oxide nanostructures; the covalent functionalization is a chemical process in which a strong bond is formed between the nanostructure material and the biological or chemical species. In most cases, some previous chemical modification of the surface is necessary to create active groups that are necessary for the binding of biological or chemical species [129, 130]. The expected sensing mechanism is based on the polarization induced bound surface charge by interaction with the ions in the liquid solutions [131].

The response of the electrochemical potential difference of the CuO nanopetals to the changes in aqueous solution of electrolyte Ag^+ was measured for a range of 1μM to 100 mM and shows that the Ag^+ dependence is linear and has sensitivity equal to 88 mV/decade at ambient conditions (Fig. 5.15 b). The linear response of the electrochemical sensor shows that the potential difference between the electrodes increases with the increase in Ag^+ concentration and it also implies that such sensor configuration can provide a large dynamical range. This linear change in the output response can be due to the large surface area and shape of the CuO nanopetals which have a significant effect to enhance the sensitivity of the working electrode.

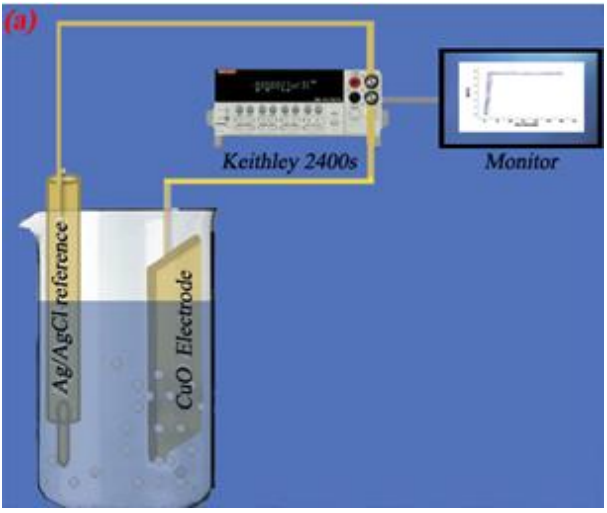

Figure 5.14: *Schematic diagram of amperometric/potentiometric measurement setup for* Ag^{+} detection.

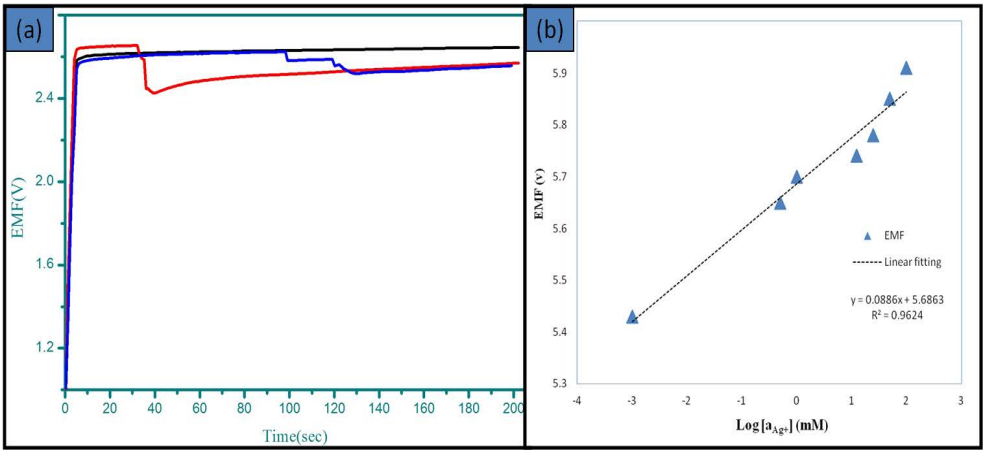

Figure 5.15: *Output response curves for the CuO nanopetals sensor at specific* Ag^{+} *concentration. The curve shows fast response, repeatable and stable output. (b) A calibration curve of the CuO nanopetals based working electrode showing the electro chemical potential difference at various* Ag^{+} *concentrations between* Ag^{+} *selective CuO nanopetals and the Ag/AgCl reference electrode.*

5.2.3 Electroluminescence (EL)

Electroluminescence (EL) phenomena was first discovered in the early 20th century by Henry Round from Marconi's Labs [132]. Electroluminescence is a non-thermal generation of light resulting from the application of electric field or driving a current through a substance, normally a semiconductor [133]. Electroluminescence is a very useful electro-optical technique which helps to understand the emission characteristics as well as the origin of the radiative centers present in the materials.

There are two types of EL devices; 1) LED devices, 2) EL devices in which light is emitted by impact excitation of a light emitting centers i.e. luminescent centers by high energy electrons (or high electric field). However our focus is on the LED in which light is generated by electron hole pair recombination in the *p-n* junction when electric current/voltage is applied. EL measurements determine the quality of the emitted light and the efficiency of the LED.

As an example, the room temperature EL spectrum of the hybrid LEDs fabricated on a paper substrate is shown in Figure 5.16 (a). The EL reveals a broad emission band covering the visible spectrum range from 420 to 780 nm. The blue shoulder peaks at 460 nm as clearly observed in the EL spectrum belongs to PFO and is attributed to the exciton emission in PFO [134]. On the other hand the EL spectrum demonstrated a broad green emission centered at 555 nm as shown in Figure 5.16 that can be ascribed to the deep level defects in ZnO. It is known that ZnO NRs grown by the solution method present a large number of defects [49]. The PFO also has a defect emission in this range due to the formation of the fluorenone agglomerates or the so called keto defect during electro- (photo) oxidation [135]. The reason for this could be the fact that when a fluorenone defect is formed, the alkyl chain is lost, favoring local interchain interaction between the PFO backbone [135]. But the presence of fluorenone defects only may not be sufficient to produce the green band emission. The interchain interactions and cross linking of the polymers are also required for the appearance of the green band [136]. These defects can

easily be produced during synthesis and functioning of the device. The peaks at 640 nm and 710 nm are frequently attributed to electrons transition within the ZnO wide bandgap, from the zinc interstitial (Zn_i) to deep oxygen interstitial (O_i) site defects [59, 137]. The emission of the device suggested that the carrier recombination takes place in the PFO/ZnO nanorods interface as recently reported [114]. The interaction between the ZnO nanorods surface and PFO molecules makes the PFO link up with ZnO. This leads to PFO/ZnO interface producing a strong defect emission [138]. As a result the device exhibits a broad EL spectrum in the range 420 nm to 780 nm and gives cold white light.

The color quality of the LED was investigated with the Commission International DE L´Eclairage (CIE). Figure 5.16(b) shows the CIE 1931 color space chromaticity diagram in the x, y coordinate system. It is clear from the chromaticity coordinates that the resultant light has a white impression with chromaticity coordinates: x = 0.4046 and y = 0.4108 and a correlated color temperature (CCT) of 3660 K for LED based on the ZnO nanorods-polymer [139, 140].

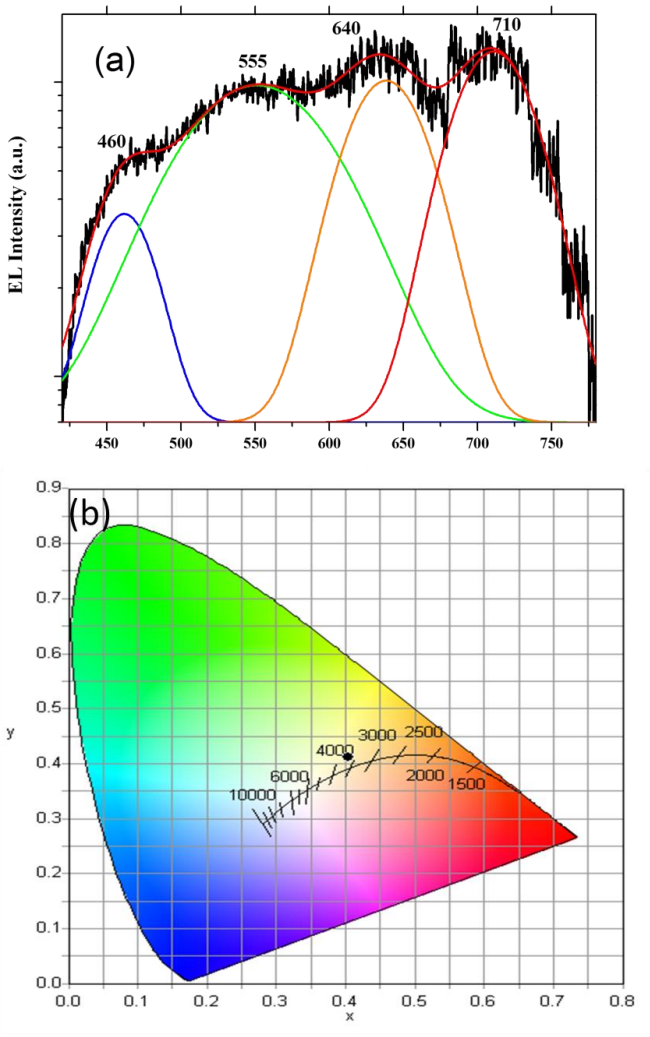

Figure 5.16:(a) *Room temperature EL spectrum obtained at 1 mA injection current and Gaussian fitting of the ZnO nanorods-polymer LED on paper substrate. (b) The CIE 1931 x, y chromaticity space, showing the chromaticity coordinates of the ZnO nanorods-polymer LED on a paper substrate[140].*

6 Conclusion and Outlook

The materials investigated here in this thesis are CuO and ZnO, which are the oxides of earth-abundant materials. A variety of ZnO and CuO nanostructures were prepared by a simple and low cost hydrothermal method. The structural, optical, electrical and sensing properties of the as deposited nanostructures have been investigated in detail. The effect of different hydrothermal conditions, especially the pH of the growth solution, growth temperature, growth time, and the precursor concentration, on the morphology and structural properties of ZnO were studied. The optimization of the growth conditions, realizing the size controllable growth and revealing the growth mechanism, has been presented for ZnO nanostructures in paper I-III. This method preserves some main advantages that it is low temperature and does not require any harsh fabrication process on the target substrates which enable the use of nonconventional substrates such as plastic, polymer, fabric and paper. Utilizing the advantages of compatibility of this method with nonconventional substrates we synthesized ZnO nanostructures on different substrates, specifically on flexible and disposable substrates, which are likely to be integrated with future foldable and disposable electronics. Low cost production is the main advantage for any product to compete in the market and ZnO nanostructures being solution processable provides much potential to become the choice for cheap devices. In addition, devices with ZnO nanorods exhibit better performance due to a better interfacial contact, having fewer defects and improved light extraction. Therefore, we have studied ZnO nanorods-based heterojuction LEDs in this work. It was possible to successfully implement ZnO nanostructures for white light emitting diodes (LEDs) on different flexible substrates. We have also extended the idea to print the ZnO nanorods hybrid LEDs to demonstrate the potential for large area and low cost flexible displays. Although devices exhibited reproducibility and had stable performance, their elevated turn-on still needs to be improved and one of the possible strategies for lowering the turn-on voltage is to improve the interface optimization and surface passivation. The efficiency measurement,

interface optimization, surface passivation, and lifetime are the key issues for the application of LED devices, and will be the focus of future work. Future efforts would also be directed to the development of printed LEDs to make even large printed area devices. The results presented in papers I-V not only provides a method for large area fabrication of ZnO nanostructures with low cost and to implement in flexible devices but also open a way to fabricate optimized nanostructures of other nanomaterials on nonconventional substrates by the hydrothermal method.

In paper VI we devoted our efforts to fabricate p-type CuO nanostructures by the same hydrothermal method and to apply them to the sensing of silver (Ag^+) ions. The fabricated sensor shows substantial advantages due to biocompatible size, low cost and simple fabrication technique. The linear potentiometric response with a slope of 88 mV/decade as a function of analyte concentration shows that the fabricated biosensor has the ability to work over a long range of ion concentration (1µM to 100 mM). In addition a rapid and stable output response for approximately 20 *sec* shows fast electrochemical reaction between the CuO nanopetals and Ag^+.

Furthermore, we have presented a novel fabrication process for the creation of low cost oxide based humidity sensor. To do this, earth abundant materials have been investigated as well as a two step hydrothermal method is used to grow n-type ZnO nanorods and p-type CuO in a sequence to form a *p-n* heterojuction. *I-V* characteristics show a typical behavior of *p-n* heterojuction for the prepared hybrid structure, which suggests that a *p-n* heterojuction of ZnO/CuO is achieved. This is the first systematic report on control growth of two different types of metal oxides and fabrication of *p-n* hetero-junction using ZnO and CuO. This structure is of great importance because it enables fabrication of humidity sensor with improved performance at very low cost, which may be a breakthrough for the development of an efficient humidity sensor. This design has also potential for cheap photovoltaic devices but to achieve all these goals further research is necessary. Efforts are still under way in our

laboratory to use those nanostructured materials for the above mentioned purposes including photovoltaic nanodevices.

7 References

[1] Wang J. Nanomaterial-based electrochemical biosensors. Analyst. 2005;130:421-6.

[2] Rodríguez JA. Synthesis, properties and applications of oxide nanomaterials. Hoboken: Wiley-Interscience; 2007.

[3] Wang ZL. Metal and semiconductor nanowires. New York, NY: Springer; 2006.

[4] Park JY, Song DE, Kim SS. An approach to fabricating chemical sensors based on ZnO nanorod arrays. Nanotechnology. 2008;19.

[5] Greene LE, Law M, Goldberger J, Kim F, Johnson JC, Zhang YF, et al. Low-temperature wafer-scale production of ZnO nanowire arrays. Angewandte Chemie-International Edition. 2003;42:3031-4.

[6] Yadav BC, Srivastava R, Dwivedi CD. Synthesis and characterization of ZnO-TiO(2) nanocomposite and its application as a humidity sensor. Philos Mag. 2008;88:1113-24.

[7] Abaker M, Umar A, Baskoutas S, Kim SH, Hwang SW. Structural and optical properties of CuO layered hexagonal discs synthesized by a low-temperature hydrothermal process. Journal of Physics D-Applied Physics. 2011;44.

[8] Song MJ, Hwang SW, Whang D. Non-enzymatic electrochemical CuO nanoflowers sensor for hydrogen peroxide detection. Talanta. 2010;80:1648-52.

[9] Banger KK, Yamashita Y, Mori K, Peterson RL, Leedham T, Rickard J, et al. Low-temperature, high-performance solution-processed metal oxide thin-film transistors formed by a 'sol-gel on chip' process. Nat Mater. 2011;10:45-50.

[10] Kim MG, Kanatzidis MG, Facchetti A, Marks TJ. Low-temperature fabrication of high-performance metal oxide thin-film electronics via combustion processing. Nat Mater. 2011;10:382-8.

[11] Michelle J.S S. Gas sensing applications of 1D-nanostructured zinc oxide: Insights from density functional theory calculations. Progress in Materials Science. 2012;57:437-86.

[12] Klingshirn CF. Zinc Oxide from fundamental properties towards novel applications. Heidelberg; London: Springer; 2010.

[13] Xu S, Wang ZL. One-dimensional ZnO nanostructures: Solution growth and functional properties. Nano Research. 2011;4:1013-98.

[14] Jagadish C, Pearton SJ. Zinc oxide bulk, thin films and nanostructures processing, properties and applications. Amsterdam; London: Elsevier; 2006.

[15] Litton CW. Zinc oxide materials for electronic and optoelectronic device applications. Chichester: Wiley; 2011.

[16] Steiner T. Semiconductor nanostructures for optoelectronic applications. Boston, Mass. [u.a.]: Artech House; 2004.

[17] Berger LI. Semiconductor materials. Boca Raton, Fla. [u.a.]: CRC Press; 1997.

[18] Sun XW, Kwok HS. Optical properties of epitaxially grown zinc oxide films on sapphire by pulsed laser deposition. J Appl Phys. 1999;86:408-11.

[19] Park YS, Schneider JR. Index of Refraction of ZnO. J Appl Phys. 1968;39:3049-52.

[20] Srikant V, Clarke DR. On the optical band gap of zinc oxide. J Appl Phys. 1998;83:5447-51.

[21] Morkoc H, Özgür U. Zinc Oxide : Fundamentals, Materials and Device Technology. Weinheim, Bergstr: WILEY-VCH; 2008.

[22] Yamazoe N, Sakai G, Shimanoe K. Oxide semiconductor gas sensors. Catal Surv Asia. 2003;7:63-75.

[23] http://enwikipediaorg/wiki/Copper(II)_oxide Access date 02/20/2012.

[24] Madelung O. Semiconductors : data handbook. Berlin ; New York: Springer; 2004.

[25] Arregui FJ. Sensors Based on Nanostructured Materials. Berlin: Springer US; 2008.

[26] Ghijsen J, Tjeng LH, Vanelp J, Eskes H, Westerink J, Sawatzky GA, et al. Electronic-Structure of Cu2o and Cuo. Phys Rev B. 1988;38:11322-30.

[27] Singh DP, Srivastava ON. Synthesis and Optical Properties of Different CuO (Ellipsoid, Ribbon and Sheet Like) Nanostructures. J Nanosci Nanotechno. 2009;9:5345-50.

[28] V M, Teixeira B, Fortunato E, Monteiro RCC, Vilarinho P. Al-doped ZnO thin films by sol-gel method. Surf Coat Tech. 2004;180:659-62.

[29] Xu ZQ, Deng H, Li Y, Guo QH, Li YR. Characteristics of Al-doped c-axis orientation ZnO thin films prepared by the sol-gel method. Mater Res Bull. 2006;41:354-8.

[30] Song K, Noh J, Jun T, Jung Y, Kang HY, Moon J. Fully Flexible Solution-Deposited ZnO Thin-Film Transistors. Advanced Materials. 2010;22:4308-+.

[31] Asif MH, Fulati A, Nur O, Willander M, Brannmark C, Stralfors P, et al. Functionalized zinc oxide nanorod with ionophore-membrane coating as an intracellular Ca[sup 2+] selective sensor. Appl Phys Lett. 2009;95:023703-3.

[32] Asif MH, Nur O, Willander M, Strålfors P, Bränmark C, Elinder F, et al. Growth and Structure of ZnO Nanorods on a Sub-Micrometer Glass Pipette and Their Application as Intracellular Potentiometric Selective Ion Sensors. Materials. 2010;3:4657-67.

[33] Asif MH, Ali SM, Nur O, Willander M, Brannmark C, Stralfors P, et al. Functionalised ZnO-nanorod-based selective electrochemical sensor for intracellular glucose. Biosens Bioelectron. 2010;25:2205-11.

[34] Round HJ. A note on carborundum. Electrical World. 1907;49:309.

[35] Holonyak N. The semiconductor p-n junction "ultimate lamp". Mrs Bull. 2005;30:515-7.

[36] Smet PF, Parmentier AB, Poelman D. Selecting Conversion Phosphors for White Light-Emitting Diodes. J Electrochem Soc. 2011;158:R37-R54.

[37] Xiang B, Wang PW, Zhang XZ, Dayeh SA, Aplin DPR, Soci C, et al. Rational synthesis of p-type zinc oxide nanowire arrays using simple chemical vapor deposition. Nano Lett. 2007;7:323-8.

[38] Chen M-T, Lu M-P, Wu Y-J, Song J, Lee C-Y, Lu M-Y, et al. Near UV LEDs Made with in Situ Doped p-n Homojunction ZnO Nanowire Arrays. Nano Lett. 2010;10:4387-93.

[39] Zhao JZ, Liang HW, Sun JC, Bian JM, Feng QJ, Hu LZ, et al. Electroluminescence from n-ZnO/p-ZnO : Sb homojunction light emitting diode on sapphire substrate with metal–organic precursors doped p-type ZnO layer grown by MOCVD technology. Journal of Physics D: Applied Physics. 2008;41:195110.

[40] Zeng YJ, Ye ZZ, Lu YF, Xu WZ, Zhu LP, Huang JY, et al. Plasma-free nitrogen doping and homojunction light-emitting diodes based on ZnO. Journal of Physics D: Applied Physics. 2008;41:165104.

[41] Baltakesmez A, Tekmen S, Tuzemen S. ZnO homojunction white light-emitting diodes. J Appl Phys. 2011;110.

[42] Mandalapu LJ, Yang Z, Chu S, Liu JL. Ultraviolet emission from Sb-doped p-type ZnO based heterojunction light-emitting diodes. Appl Phys Lett. 2008;92.

[43] Hsu YF, Xi YY, Tam KH, Djurisic AB, Luo JM, Ling CC, et al. Undoped p-type ZnO nanorods synthesized by a hydrothermal method. Adv Funct Mater. 2008;18:1020-30.

[44] Ohta H, Kawamura K, Orita M, Hirano M, Sarukura N, Hosono H. Current injection emission from a transparent p-n junction composed of p-SrCu2O2/n-ZnO. Appl Phys Lett. 2000;77:475-7.

[45] Ozgur U, Alivov YI, Liu C, Teke A, Reshchikov MA, Dogan S, et al. A comprehensive review of ZnO materials and devices. J Appl Phys. 2005;98:041301-103.

[46] Lai E, Kim W, Yang PD. Vertical Nanowire Array-Based Light Emitting Diodes. Nano Research. 2008;1:123-8.

[47] Jeong MC, Oh BY, Ham MH, Lee SW, Myoung JM. ZnO-Nanowire-Inserted GaN/ZnO heterojunction light-emitting diodes. Small. 2007;3:568-72.

[48] Willander M, Nur O, Zhao QX, Yang LL, Lorenz M, Cao BQ, et al. Zinc oxide nanorod based photonic devices: recent progress in growth, light emitting diodes and lasers. Nanotechnology. 2009;20:332001.

[49] Djurisic AB, Leung YH. Optical properties of ZnO nanostructures. Small. 2006;2:944-61.

[50] Travlos A, Boukos N, Chandrinou C. Zinc related defects in ZnO nanorods. physica status solidi (b). 2012;249:560-3.

[51] Lupan O, Pauporte T, Viana B. Low-Voltage UV-Electroluminescence from ZnO-Nanowire Array/p-GaN Light-Emitting Diodes. Advanced Materials. 2010;22:3298-+.

[52] Alvi NH, Riaz M, Tzamalis G, Nur O, Willander M. Fabrication and characterization of high-brightness light emitting diodes based on n-ZnO nanorods grown by a low-temperature chemical method on p-4H-SiC and p-GaN. Semicond Sci Tech. 2010;25.

[53] Son DI, You CH, Kim WT, Kim TW. White light-emitting diodes fabricated utilizing hybrid polymer-colloidal ZnO quantum dots. Nanotechnology. 2009;20.

[54] Liu J, Ahn YH, Park JY, Koh KH, Lee S. Hybrid light-emitting diodes based on flexible sheets of mass-produced ZnO nanowires. Nanotechnology. 2009;20.

[55] Sun XW, Huang JZ, Wang JX, Xu Z. A ZnO nanorod inorganic/organic heterostructure light-emitting diode emitting at 342 nm. Nano Lett. 2008;8:1219-23.

[56] Shariffudin SS, Rahim MHIA, Zulkifli Z, Hamzah AS, Rusop M. Optical Properties of Nanocomposite MEH-PPV:ZnO Thin Films. Aip Conf Proc. 2011;1341:358-61.

[57] Wang D-W, Zhao S-L, Xu Z, Kong C, Gong W. The improvement of near-ultraviolet electroluminescence of ZnO nanorods/MEH-PPV heterostructure by using a ZnS buffer layer. Organic Electronics. 2011;12:92-7.

[58] Bano N, Zaman S, Zainelabdin A, Hussain S, Hussain I, Nur O, et al. ZnO-organic hybrid white light emitting diodes grown on flexible plastic using low temperature aqueous chemical method. J Appl Phys. 2010;108.

[59] Zainelabdin A, Zaman S, Amin G, Nur O, Willander M. Stable White Light Electroluminescence from Highly Flexible Polymer/ZnO Nanorods Hybrid Heterojunction Grown at 50°C. Nanoscale Res Lett. 2010;5:1442-8.

[60] Zaman S, Zainelabdin A, Amin G, Nur O, Willander M. Effect of the polymer emission on the electroluminescence characteristics of n-ZnO nanorods/p-polymer hybrid light emitting diode. Applied Physics A. 2011.

[61] Yip H-L, Hau SK, Baek NS, Jen AKY. Self-assembled monolayer modified ZnO/metal bilayer cathodes for polymer/fullerene bulk-heterojunction solar cells. Appl Phys Lett. 2008;92:193313-3.

[62] Khan AA, Khalid M. Synthesis of Nano-Sized ZnO and Polyaniline-Zinc Oxide Composite: Characterization, Stability in Terms of DC Electrical Conductivity Retention and Application in Ammonia Vapor Detection. J Appl Polym Sci. 2010;117:1601-7.

[63] Nadarajah A, Word RC, Meiss J, Konenkamp R. Flexible inorganic nanowire light-emitting diode. Nano Lett. 2008;8:534-7.

[64] Konenkamp R, Word RC, Godinez M. Ultraviolet electroluminescence from ZnO/polymer heterojunction light-emitting diodes. Nano Lett. 2005;5:2005-8.

[65] Konenkamp R, Word RC, Schlegel C. Vertical nanowire light-emitting diode. Appl Phys Lett. 2004;85:6004-6.

[66] Bolink HJ, Coronado E, Sessolo M. White Hybrid Organic-Inorganic Light-Emitting Diode Using ZnO as the Air-Stable Cathode. Chem Mater. 2009;21:439-41.

[67] Bolink HJ, Coronado E, Orozco J, Sessolo M. Efficient Polymer Light-Emitting Diode Using Air-Stable Metal Oxides as Electrodes. Advanced Materials. 2009;21:79-82.

[68] Bolink HJ, Coronado E, Repetto D, Sessolo M. Air stable hybrid organic-inorganic light emitting diodes using ZnO as the cathode. Appl Phys Lett. 2007;91.

[69] Willander M, Nur O, Zaman S, Zainelabdin A, Amin G, Sadaf JR, et al. Intrinsic white-light emission from zinc oxide nanorods heterojunctions on large-area substrates. 2011:79400A-A-10.

[70] Solanki PR, Kaushik A, Agrawal VV, Malhotra BD. Nanostructured metal oxide-based biosensors. Npg Asia Mater. 2011;3:17-24.

[71] Eggins BR. Chemical sensors and biosensors. Chichester [u.a.]: Wiley; 2002.

[72] Asif MH, Ali SMU, Nur O, Willander M, Brannmark C, Stralfors P, et al. Functionalised ZnO-nanorod-based selective electrochemical sensor for intracellular glucose. Biosens Bioelectron. 2010;25:2205-11.

[73] Asif MH, Nur O, Willander M, Danielsson B. Selective calcium ion detection with functionalized ZnO nanorods-extended gate MOSFET. Biosens Bioelectron. 2009;24:3379-82.

[74] Patolsky F, Lieber CM. Nanowire nanosensors. Materials Today. 2005;8:20-8.

[75] Rahman MM, Ahammad AJS, Jin JH, Ahn SJ, Lee JJ. A Comprehensive Review of Glucose Biosensors Based on Nanostructured Metal-Oxides. Sensors-Basel. 2010;10:4855-86.

[76] Ibupoto ZH, Ali SMU, Chey CO, Khun K, Nur O, Willander M. Selective zinc ion detection by functionalised ZnO nanorods with ionophore. J Appl Phys. 2011;110.

[77] Bakker E, Buhlmann P, Pretsch E. Polymer membrane ion-selective electrodes - What are the limits. Electroanal. 1999;11:915-33.

[78] Buhlmann P, Pretsch E, Bakker E. Carrier-based ion-selective electrodes and bulk optodes. 2. Ionophores for potentiometric and optical sensors. Chem Rev. 1998;98:1593-687.

[79] Asif M. Zinc Oxide Nanostructure Based Electrochemical Sensors and Drug Delivery to Intracellular Environments [Doctoral thesis (PhD)]. Linköping University Electronic Press: Linköping; 2011.

[80] Sakai Y, Sadaoka Y, Matsuguchi M. Humidity sensors based on polymer thin films. Sensor Actuat B-Chem. 1996;35:85-90.

[81] Chang S-P, Chang S-J, Lu C-Y, Li M-J, Hsu C-L, Chiou Y-Z, et al. A ZnO nanowire-based humidity sensor. Superlattice Microst. 2010;47:772-8.

[82] Cantalini C, Pelino M. Microstructure and Humidity-Sensitive Characteristics of Alpha-Fe2o3 Ceramic Sensor. Journal of the American Ceramic Society. 1992;75:546-51.

[83] Li MQ, Chen YF. An investigation of response time of TiO2 thin-film oxygen sensors. Sensor Actuat B-Chem. 1996;32:83-5.

[84] Biju KP, Jain MK. Effect of crystallization on humidity sensing properties of sol-gel derived nanocrystalline TiO2 thin films. Thin Solid Films. 2008;516:2175-80.

[85] Chauhan P, Annapoorni S, Trikha SK. Humidity-sensing properties of nanocrystalline haematite thin films prepared by sol-gel processing. Thin Solid Films. 1999;346:266-8.

[86] Chang SP, Chang SJ, Lu CY, Li MJ, Hsu CL, Chiou YZ, et al. A ZnO nanowire-based humidity sensor. Superlattice Microst. 2010;47:772-8.

[87] Wang Y, Yeow JTW, Yin YT, Chen LY. Fabricating ZnO nanowires-based Humidity Sensor via Dielectrophoresis Method. Inec: 2010 3rd International Nanoelectronics Conference, Vols 1 and 2. 2010:446-7.

[88] Qi Q, Zhang T, Yu QJ, Wang R, Zeng Y, Liu L, et al. Properties of humidity sensing ZnO nanorods-base sensor fabricated by screen-printing. Sensor Actuat B-Chem. 2008;133:638-43.

[89] Dixit S, Srivastava A, Shukla RK, Srivastava A. ZnO thick film based opto-electronic humidity sensor for a wide range of humidity. Opt Rev. 2007;14:186-8.

[90] Yuan CH, Xu YT, Deng YM, Jiang NN, He N, Dai LZ. CuO based inorganic-organic hybrid nanowires: a new type of highly sensitive humidity sensor. Nanotechnology. 2010;21.

[91] Nakamura Y, Ando A, Tsurutani T, Okada O, Miyayama M, Koumoto K, et al. Gas Sensitivity of Cuo/Zno Hetero-Contact. Chem Lett. 1986:413-6.

[92] Yoo DJ, Park SJ. Electrolysis of water in CuO/ZnO heterocontact humidity sensor. J Electrochem Soc. 1996;143:L89-L91.

[93] Ushio Y, Miyayama M, Yanagida H. Fabrication of thin-film CuO/ZnO heterojunction and its humidity-sensing properties. Sensors and Actuators B: Chemical. 1993;12:135-9.

[94] Yu JH, Choi GM. Current-voltage characteristics and selective CO detection of Zn2SnO4 and ZnO/Zn2SnO4, SnO2/Zn2SnO4 layered-type sensors. Sensor Actuat B-Chem. 2001;72:141-8.

[95] Yu JH, Choi GM. Selective CO gas detection of CuO- and ZnO-doped SnO2 gas sensor. Sensor Actuat B-Chem. 2001;75:56-61.

[96] Kulwicki BM. Humidity Sensors. Journal of the American Ceramic Society. 1991;74:697-708.

[97] Greene LE, Law M, Tan DH, Montano M, Goldberger J, Somorjai G, et al. General route to vertical ZnO nanowire arrays using textured ZnO seeds. Nano Lett. 2005;5:1231-6.

[98] Pacholski C, Kornowski A, Weller H. Self-assembly of ZnO: from nanodots to nanorods. Angew Chem Int Ed Engl. 2002;41:1188-91.

[99] Amin G, Asif MH, Zainelabdin A, Zaman S, Nur O, Willander M. Influence of pH, precursor concentration, growth time, and temperature on the morphology of ZnO nanostructures grown by the hydrothermal method. Journal of Nanomaterials. 2011;2011.

[100] Vayssieres L, Keis K, Lindquist SE, Hagfeldt A. Purpose-built anisotropic metal oxide material: 3D highly oriented microrod array of ZnO. J Phys Chem B. 2001;105:3350-2.

[101] Wang ZL. Zinc oxide nanostructures: growth, properties and applications. Journal of Physics-Condensed Matter. 2004;16:R829-R58.

[102] Wang ZL, Xu S, Lao C, Weintraub B. Density-controlled growth of aligned ZnO nanowire arrays by seedless chemical approach on smooth surfaces. Journal of Materials Research. 2008;23:2072-7.

[103] Willander M, Ul Hasan K, Nur O, Zainelabdin A, Zaman S, Amin G. Recent progress on growth and device development of ZnO and CuO nanostructures and graphene nanosheets. Journal of Materials Chemistry. 2012;22:2337-50.

[104] Ko SH, Lee D, Kang HW, Nam KH, Yeo JY, Hong SJ, et al. Nanoforest of hydrothermally grown hierarchical ZnO nanowires for a high efficiency dye-sensitized solar cell. Nano Lett. 2011;11:666-71.

[105] Zainelabdin A, Zaman S, Amin G, Nur O, Willander M. Deposition of Well-Aligned ZnO Nanorods at 50 degrees C on Metal, Semiconducting Polymer, and Copper Oxides Substrates and Their Structural and Optical Properties. Cryst Growth Des. 2010;10:3250-6.

[106] Amin G, Hussain I, Zaman S, Bano N, Nur O, Willander M. Current-transport studies and trap extraction of hydrothermally grown ZnO nanotubes using gold Schottky diode. physica status solidi (a). 2010;207:748-52.

[107] Israr MQ, Sadaf JR, Yang LL, Nur O, Willander M, Palisaitis J, et al. Trimming of aqueous chemically grown ZnO nanorods into ZnO nanotubes and their comparative optical properties. Appl Phys Lett. 2009;95.

[108] Amin G, Asif MH, Zainelabdin A, Zaman S, Nur O, Willander M. Influence of pH, Precursor Concentration, Growth Time, and Temperature on the Morphology of ZnO Nanostructures Grown by the Hydrothermal Method. Journal of Nanomaterials. 2011;2011:1-9.

[109] Guo X, Guo M, Zhang M, Wang X, Chou K-C. Effects of pretreatment of substrates on the preparation of large scale ZnO nanotube arrays. Rare Metals. 2010;29:21-5.

[110] Sadaf JR, Israr MQ, Kishwar S, Nur O, Willander M. White Electroluminescence Using ZnO Nanotubes/GaN Heterostructure Light-Emitting Diode. Nanoscale Res Lett. 2010;5:957-60.

[111] Vayssieres L. Growth of Arrayed Nanorods and Nanowires of ZnO from Aqueous Solutions. Advanced Materials. 2003;15:464-6.

[112] Zhang XJ, Gu AX, Wang GF, Wang W, Wu HQ, Fang B. Seed-mediated Preparation of CuO Nanoflowers and their Application as Hydrazine Sensor. Chem Lett. 2009;38:466-7.

[113] Choi JD, Choi GM. Electrical and CO gas sensing properties of layered ZnO-CuO sensor. Sensor Actuat B-Chem. 2000;69:120-6.

[114] Wadeasa A, Tzamalis G, Sehati P, Nur O, Fahlman M, Willander M, et al. Solution processed ZnO nanowires/polyfluorene heterojunctions for large area lightening. Chemical Physics Letters. 2010;490:200-4.

[115] Amin G, Sandberg MO, Zainelabdin A, Zaman S, Nur O, Willander M. Scale-up synthesis of ZnO nanorods for printing inexpensive ZnO/polymer white light-emitting diode. Journal of Materials Science. 2012:1-6.

[116] Goldstein J. Scanning electron microscopy and x-ray microanalysis. New York: Kluwer Academic/Plenum Publishers; 2003.

[117] Zhou W. Advanced scanning microscopy for nanotechnology techniques and applications. New York, NY: Springer; 2007.

[118] Atteberry J. http://science.howstuffworks.com/scanning-electron-microscope.htm Access date 03/28/2012.

[119] TEM. http://materialcerdas.wordpress.com/teori-dasar/transmission-electron-microscopy-tem. Access date 03/28/2012.

[120] Zhong Q, Inniss D, Kjoller K, Elings VB. Fractured polymer/silica fiber surface studied by tapping mode atomic force microscopy. Surface Science Letters. 1993;290:L688-L92.

[121] Geisse NA. AFM and combined optical techniques. Materials Today. 2009;12:40-5.

[122] AFM. http://www.microbiologybytes.com/blog/2010/07/20/microbial-nanoscopy/Access Access date 04/09/2012.
.

[123] Zaman S, Asif MH, Zainelabdin A, Amin G, Nur O, Willander M. CuO nanoflowers as an electrochemical pH sensor and the effect of pH on the growth. J Electroanal Chem. 2011;662:421-5.

[124] Chen XD, Ling CC, Fung S, Beling CD, Mei YF, Fu RKY, et al. Current transport studies of ZnO/p-Si heterostructures grown by plasma immersion ion implantation and deposition. Appl Phys Lett. 2006;88:132104-3.

[125] Carrier-transport studies of III-nitride/Si3N4/Si isotype heterojunctions. physica status solidi (a). 2012:n/a.

[126] Electrical-optical properties of nanofiber ZnO film grown by sol gel method and fabrication of ZnO/p-Si heterojunction. Solid State Sciences. 2011.

[127] Amin G, Hussain I, Zaman S, Bano N, Nur O, Willander M. Current-transport studies and trap extraction of hydrothermally grown ZnO nanotubes using gold Schottky diode. Phys Status Solidi A. 2010;207:748-52.

[128] Ali SMU, Asif MH, Fulati A, Nur O, Willander M, Brannmark C, et al. Intracellular K(+) Determination With a Potentiometric Microelectrode Based on ZnO Nanowires. Ieee T Nanotechnol. 2011;10:913-9.

[129] Asif MH, Nur O, Willander M, Stralfors P, Brannmark C, Elinder F, et al. Growth and Structure of ZnO Nanorods on a Sub-Micrometer Glass Pipette and Their Application as Intracellular Potentiometric Selective Ion Sensors. Materials. 2010;3:4657-67.

[130] Asif MH, Nur O, Willander M, Danielsson B. Selective calcium ion detection with functionalized ZnO nanorods-extended gate MOSFET. Biosens Bioelectron. 2009;24:3379-82.

[131] Asif MH, Fulati A, Nur O, Willander M, Brannmark C, Stralfors P, et al. Functionalized zinc oxide nanorod with ionophore-membrane coating as an intracellular Ca(2+) selective sensor. Appl Phys Lett. 2009;95.

[132] Chen NP. Handbook of light emitting and Schottky diode research. New York: Nova Science Publishers; 2009.

[133] Ono YA. Electroluminescent displays. Singapore [u.a.]: World Scientific; 1995.

[134] Wadeasa A, Nur O, Willander M. The effect of the interlayer design on the electroluminescence and electrical properties of n-ZnO nanorod/p-type blended polymer hybrid light emitting diodes. Nanotechnology. 2009;20:065710.

[135] Montilla F, Mallavia R. On the origin of green emission bands in fluorene-based conjugated polymers. Adv Funct Mater. 2007;17:71-8.

[136] Zhao W, Cao T, White JM. On the origin of green emission in polyfluorene polymers: The roles of thermal oxidation degradation and crosslinking. Adv Funct Mater. 2004;14:783-90.

[137] Zainelabdin A, Zaman S, Amin G, Nur O, Willander M. Deposition of Well-Aligned ZnO Nanorods at 50 °C on Metal, Semiconducting Polymer, and Copper Oxides Substrates and Their Structural and Optical Properties. Cryst Growth Des. 2010;10:3250-6.

[138] Lee CY, Wang JY, Chou Y, Cheng CL, Chao CH, Shiu SC, et al. White-light electroluminescence from ZnO nanorods/polyfluorene by solution-based growth. Nanotechnology. 2009;20.

[139] Alvi NH, Usman Ali SM, Hussain S, Nur O, Willander M. Fabrication and comparative optical characterization of n-ZnO nanostructures (nanowalls, nanorods, nanoflowers and nanotubes)/p-GaN white-light-emitting diodes. Scripta Materialia. 2011;64:697-700.

[140] Amin G, Zaman S, Zainelabdin A, Nur O, Willander M. ZnO nanorods-polymer hybrid white light emitting diode grown on a disposable paper substrate. Physica Status Solidi-Rapid Research Letters. 2011;5:71-3.

Notes

Notes

Notes

Notes